Large scale applications:

* **Verwey transition (magnetite, $YBaFe_2O_5$)**
* **Boron nitride BN on** transition metal **(111) surfaces**
* **Misfit layer compounds $PbS_{1.14}TaS_2$**

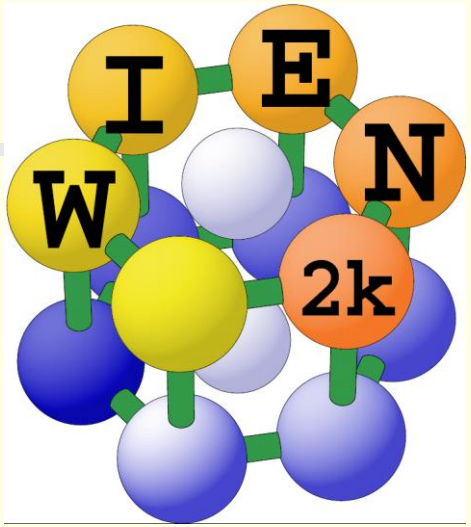

Karlheinz Schwarz

Institut für Materialchemie

TU Wien

1. example: $YBaFe_2O_5$

Magnetic and charge order phase transition in

$YBaFe_2O_5$ (Verwey transition)

Thanks to: Pavel Karen (Univ. Oslo, Norway)

E.Verwey, Nature 144, 327 (1939)

Fe_3O_4, magnetite

phase transition between a **mixed-valence** and a **charge-ordered** configuration

$$2\ Fe^{2.5+} \rightarrow Fe^{2+} + Fe^{3+}$$

cubic inverse spinel structure AB_2O_4

~~$Fe^{2+}_A (Fe^{3+},Fe^{3+})_B O_4$~~

$Fe^{3+}_A (Fe^{2+},Fe^{3+})_B O_4$

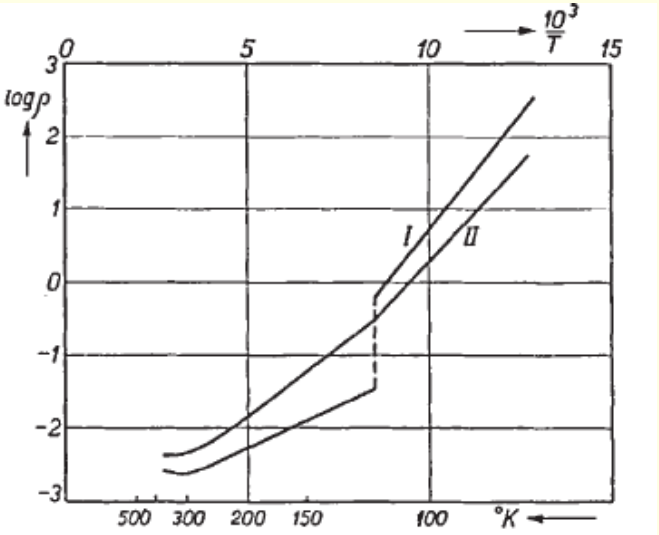

The accompanying graph shows log ρ against $1/T$ for two bars: I with $FeO : Fe_2O_3 = 1 : 1{\cdot}025$, and II with $FeO : Fe_2O_3 = 1 : 1{\cdot}08$. All details of the curves are in full accordance with the picture proposed above for the nature of the transition and our concept of the cation arrangement in the Fe_3O_4 (and the γ-Fe_2O_3) lattice. In further support of our views, we found that sample I shows a distinct drop in the susceptibility for weak magnetic fields at about 117° K., whereas with sample II the corresponding effect is much weaker.

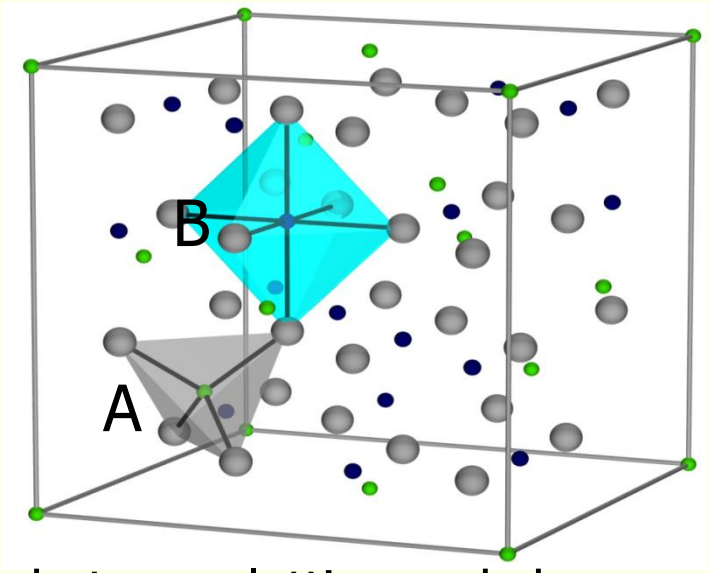

→ small, but complicated coupling between lattice and charge order

… as a B-site Fe network

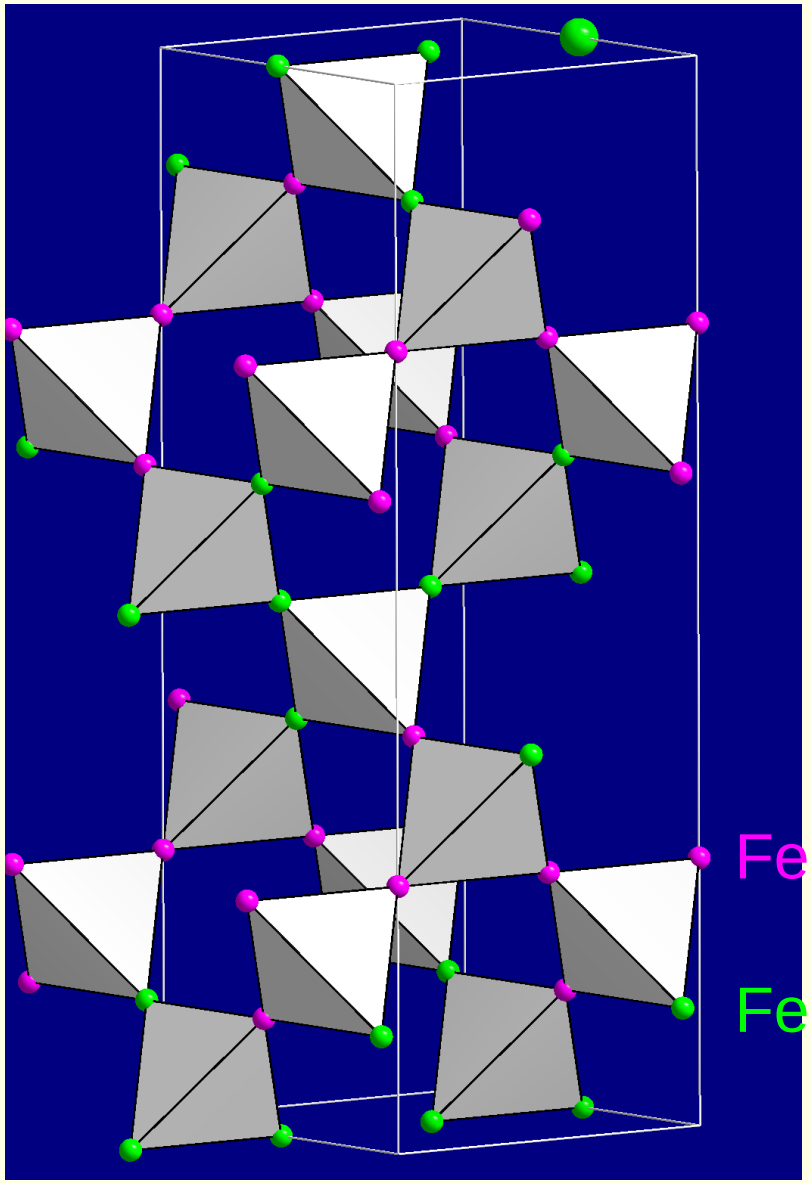

3+1 order

Verwey suggestion:

Verwey et al. *J.Chem.Phys* **15**(1947)181

Imma

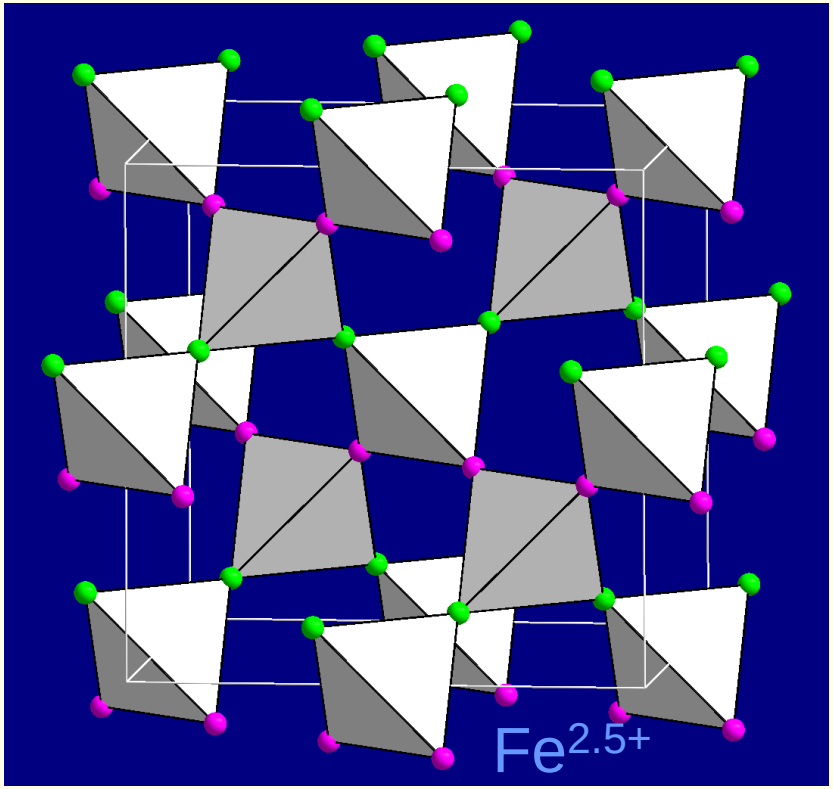

2+2 order minimizes nearest-neighbor Coulombic energy

Wright *et al*. *PRB* **66** (2002) 214422

P.W.Anderson, *PR* **102** (1956)1008

Double-cell perovskites: $RBaFe_2O_5$

ABO_3

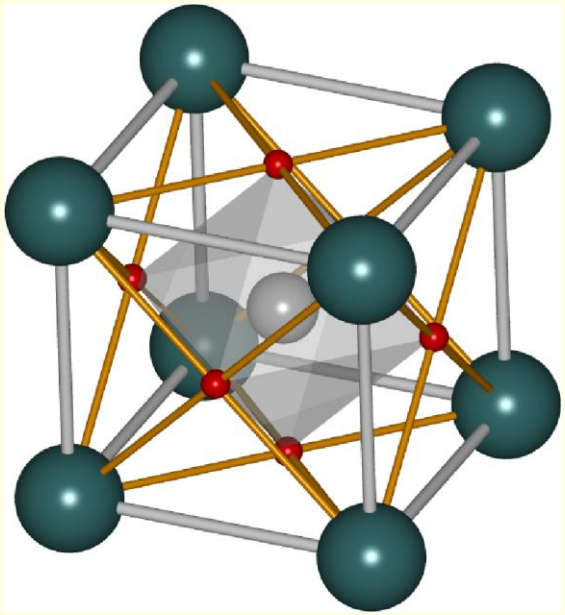

O-deficient **double-perovskite**

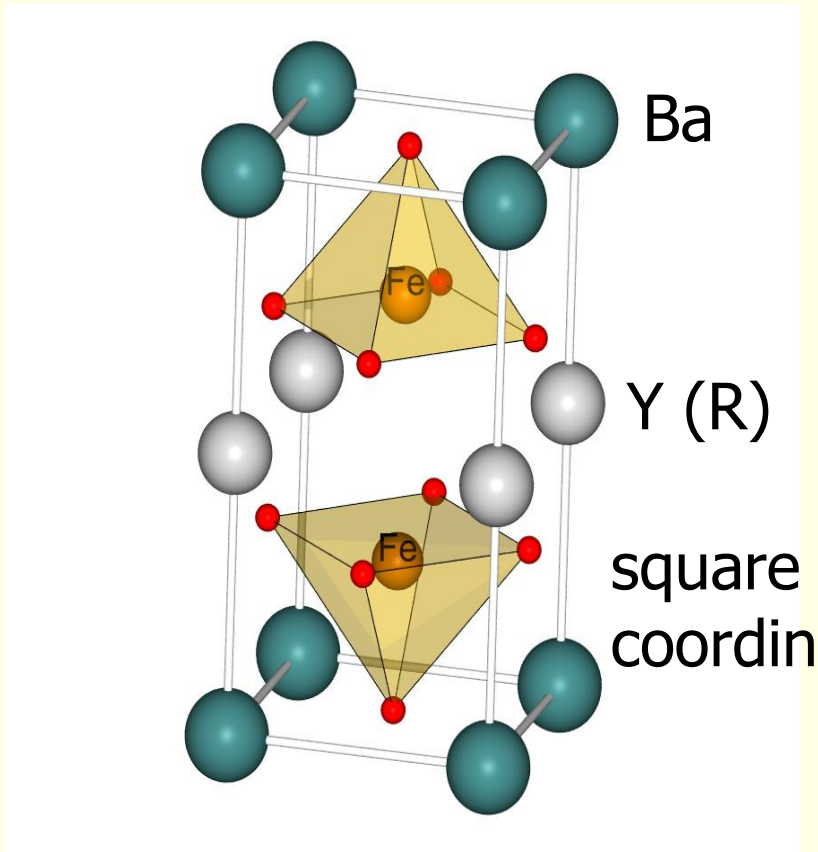

Antiferromagnet with a 2 step Verwey transition around 300 K

Woodward&Karen, Inorganic Chemistry 42, 1121 (2003)

structural changes

CO structure: Pmma

a:b:c=2.09:1:1.96 (20K)

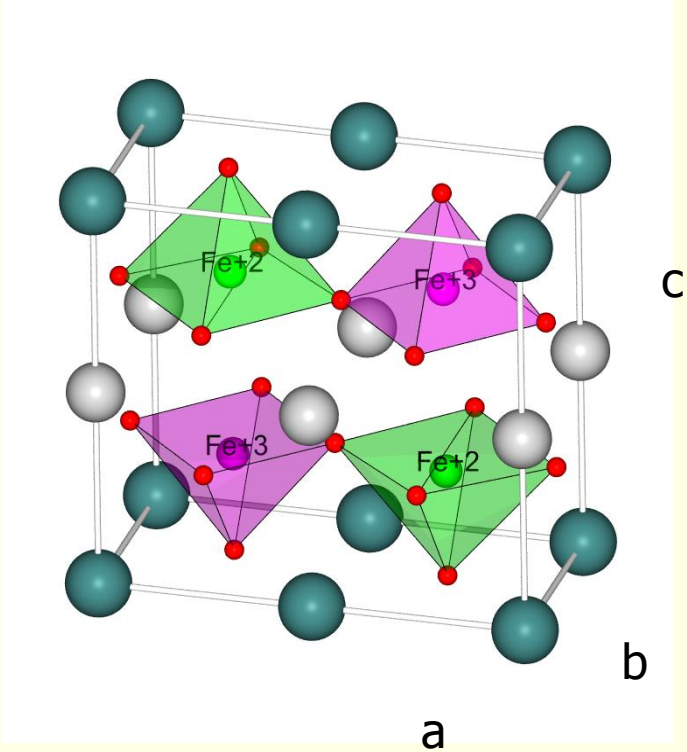

VM structure: Pmmm

a:b:c=1.003:1:1.93 (340K)

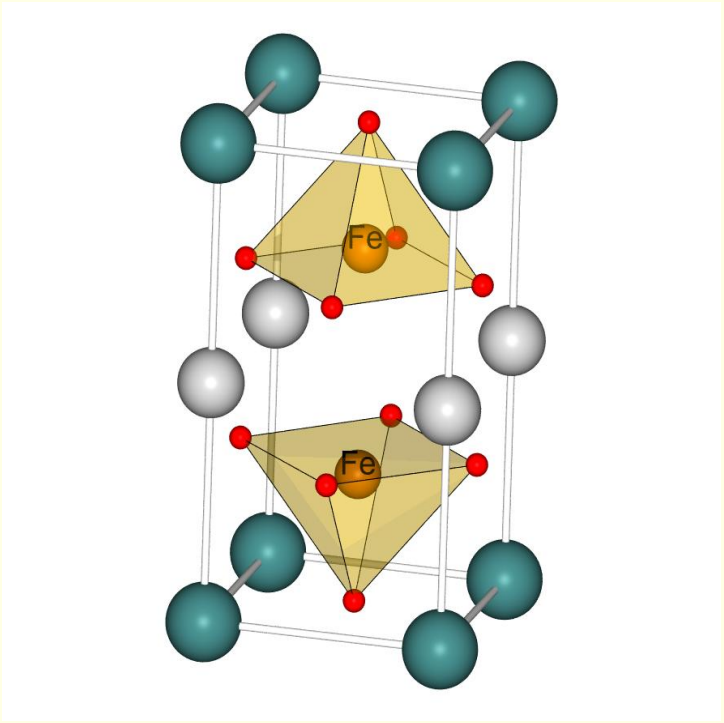

- Fe^{2+} and Fe^{3+} chains along b
- contradicts Anderson charge-ordering conditions with minimal electrostatic repulsion (checkerboard like pattern)
- has to be compensated by orbital ordering and e^--lattice coupling

antiferromagnetic structure

CO phase: G-type AFM

- AFM arrangement in all directions, also across Y-layer
- Fe moments in b-direction

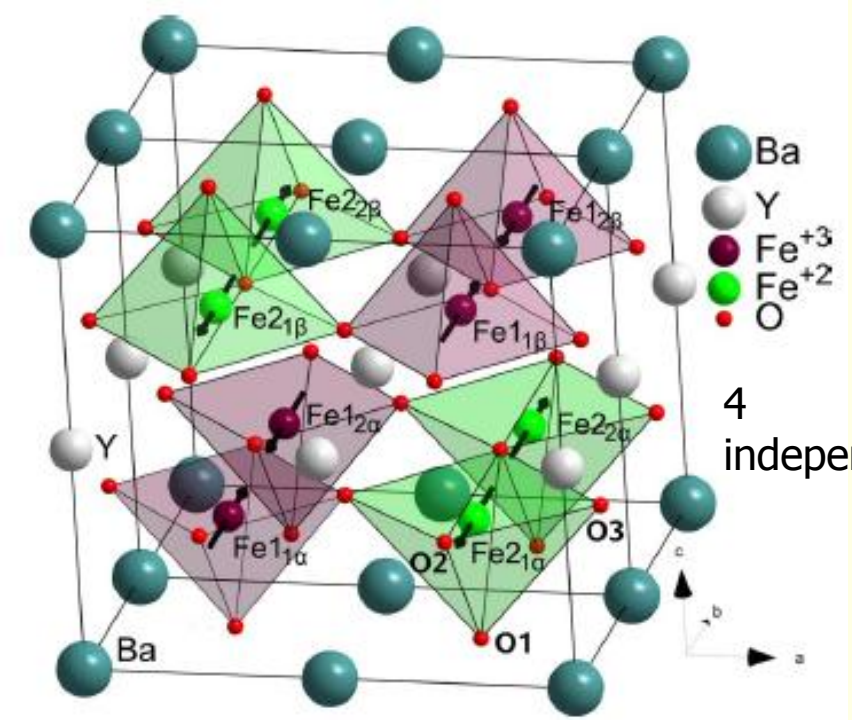

FIG. 1. (Color online) The magnetic 1×2×1 CO supercell. The arrows depict the direction of the magnetic moments.

4 8 independent Fe atoms

VM phase:

AFM for all Fe-O-Fe superexchange paths
FM across Y-layer (direct Fe-Fe exchange)

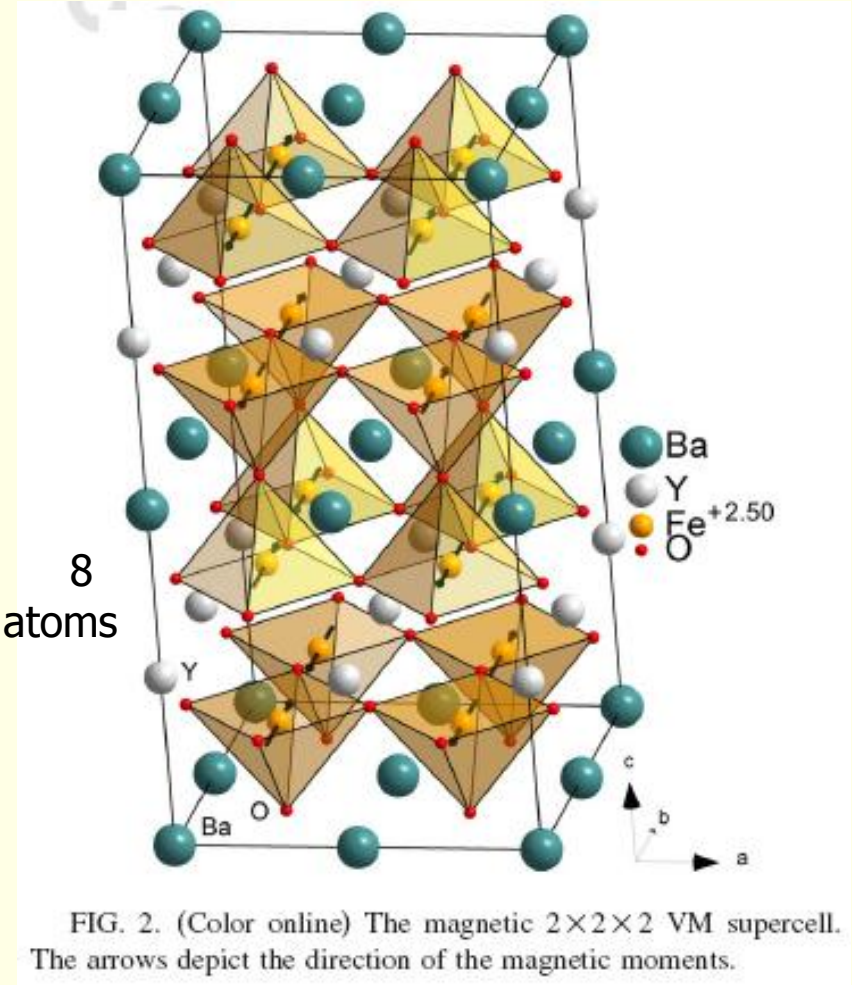

FIG. 2. (Color online) The magnetic 2×2×2 VM supercell. The arrows depict the direction of the magnetic moments.

"Localized electrons": GGA+U

- Hybrid-DFT
  - $E_{xc}^{PBE0}[\rho] = E_{xc}^{PBE}[\rho] + \alpha\,(E_x^{HF}[\Phi_{sel}] - E_x^{PBE}[\rho_{sel}])$
- LDA+U, GGA+U
  - $E^{LDA+U}(\rho,n) = E^{LDA}(\rho) + E^{orb}(n) - E^{DCC}(\rho)$
    - separate electrons into "itinerant" (LDA) and localized e^- (TM-3d, RE 4f e^-)
    - treat them with "approximate screened Hartree-Fock"
    - correct for "double counting"

$$E^{orb}(\hat{n}) = \frac{U}{2}\sum_{m,m',\sigma}\hat{n}_{m\sigma}\hat{n}_{m'-\sigma} + \frac{U-J}{2}\sum_{m\neq m',\sigma}\hat{n}_{m\sigma}\hat{n}_{m'\sigma}$$

  - Hubbard-U describes coulomb energy for $2e^-$ at the same site

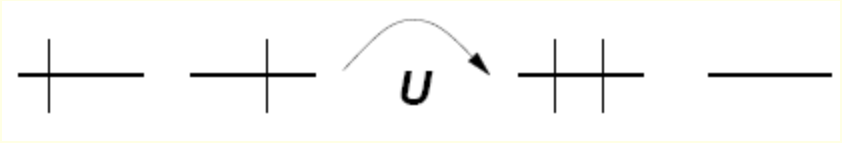

  - orbital dependent potential

$$V_{m,m',\sigma} = (U-J)(\tfrac{1}{2} - n_{m,m',\sigma})$$

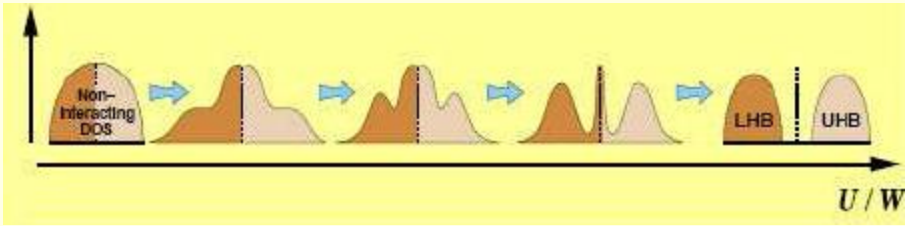

GGA-results:

- ***Metallic** behaviour/No bandgap*
  - Fe-dn t_{2g} states not splitted at E_F
  - overestimated covalency between O-p and Fe-e_g
- *Magnetic moments too small*
  - Experiment:
    - CO: 4.15/3.65 (for Tb), 3.82 (av. for Y)
    - VM: ~3.90
  - Calculation:
    - CO: 3.37/3.02
    - VM: 3.34
- *no significant charge order*
  - charges of Fe^{2+} and Fe^{3+} sites nearly identical
- *CO phase less stable than VM*
- ***LDA/GGA NOT suited for this compound!***

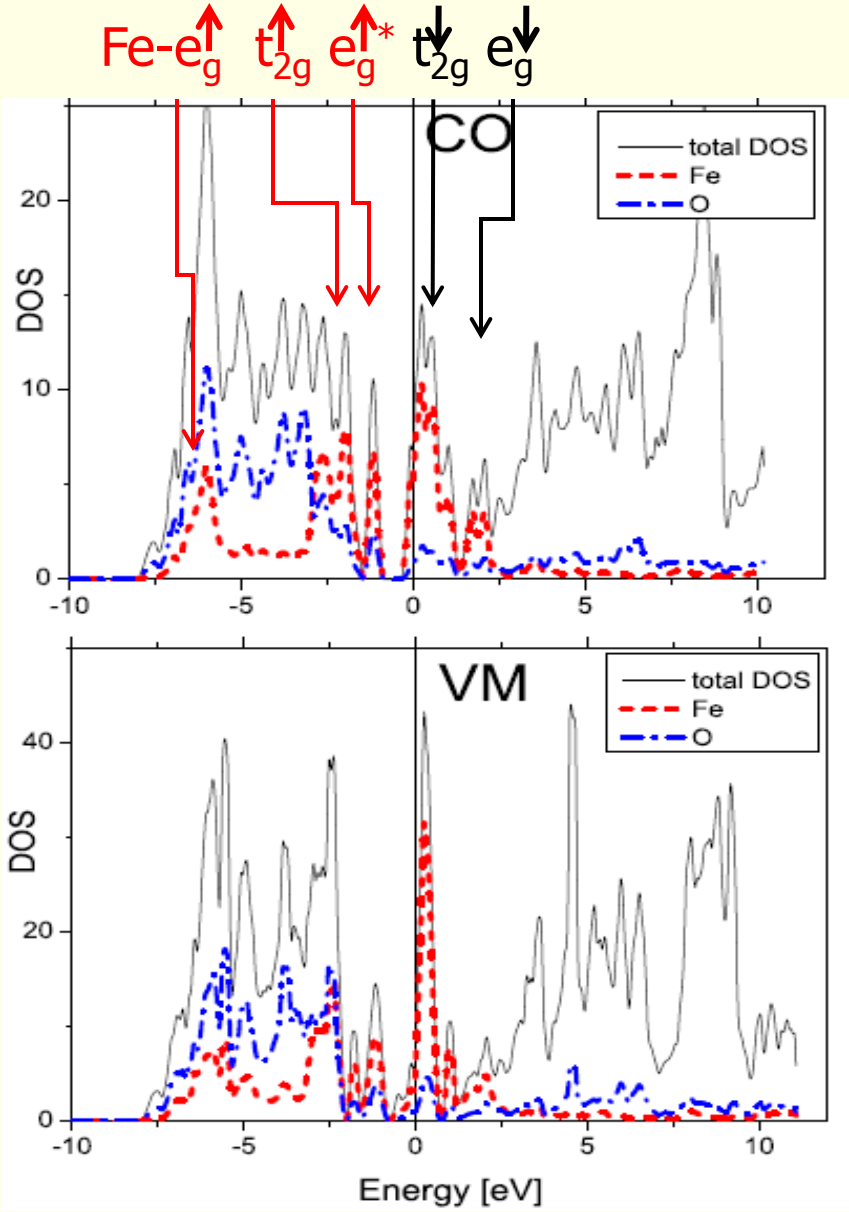

DOS: GGA+U vs. GGA

GGA+U

GGA

single lower Hubbard-band in VM splits in CO with Fe^{3+} states lower than Fe^{2+}

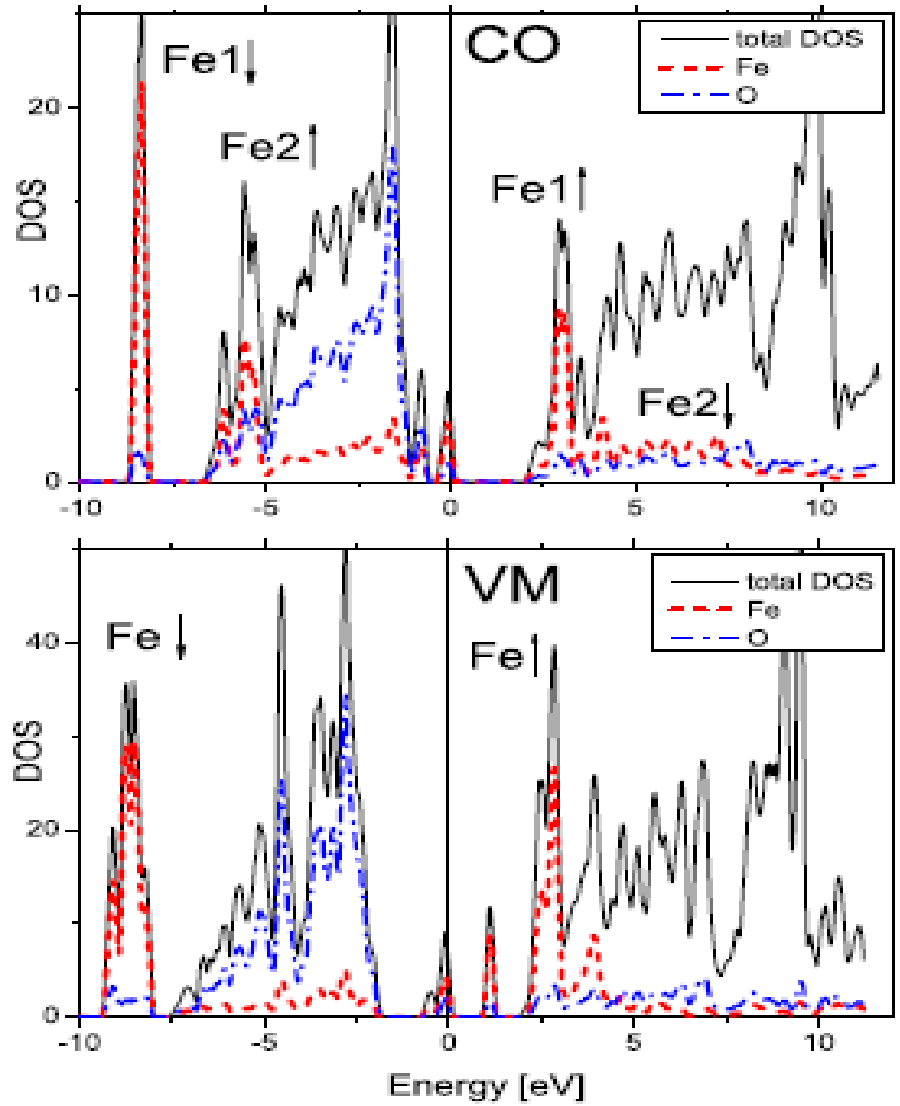

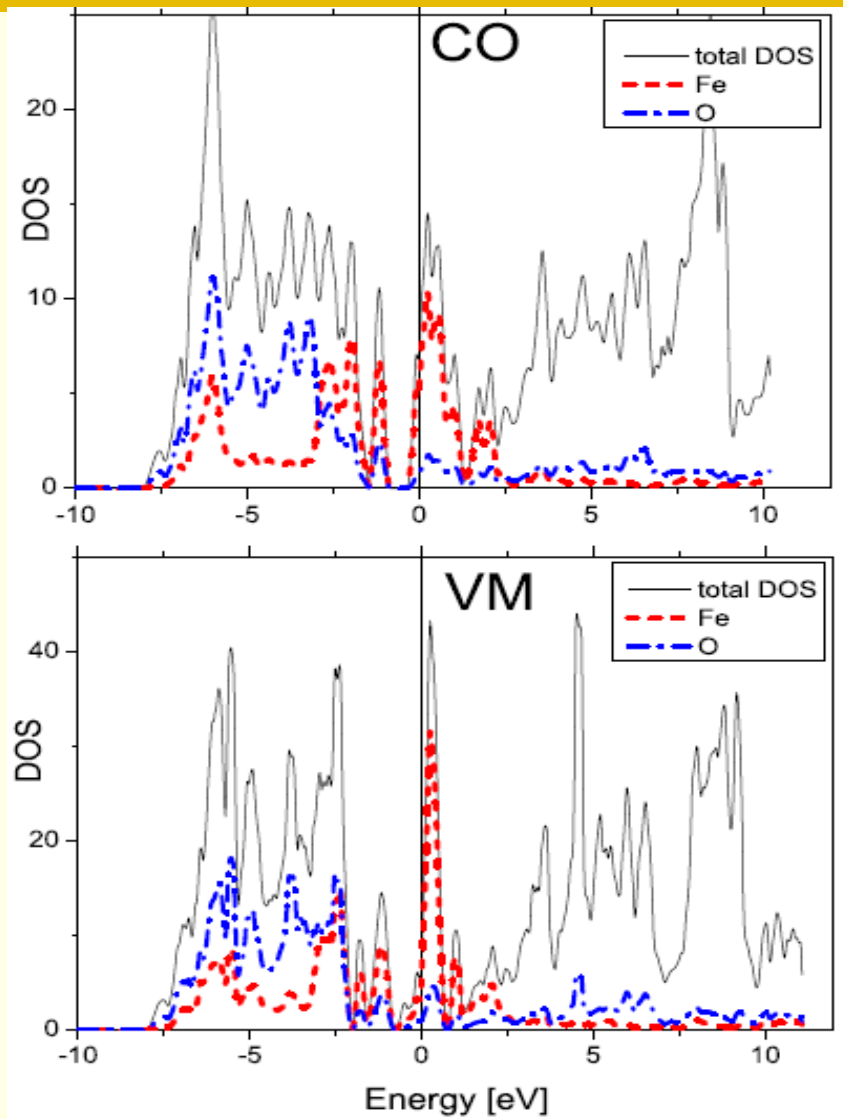

magnetic moments and band gap

TABLE V: Dependence of the band gap (in eV), the orbital μ_{orb}, spin μ_S and total moments μ_{tot} (in μ_B) on U_{eff} for the CO and VM phases. Experimental values are taken from ref.[7].

	CO					VM				
	exp.	U_{eff} [eV]				exp.	U_{eff} [eV]			
	—	5	6	7	8	—	5	6	7	8
μ_{orb} $Fe1^{3+}$	—	0.01	0.01	0.01	0.01	—	0.05	0.05	0.04	0.04
μ_{orb} $Fe2^{2+}$	—	0.10	0.10	0.12	0.11					
μ_S $Fe1^{3+}$	—	3.95	4.02	4.07	4.14	—	3.81	3.87	3.92	3.97
μ_S $Fe2^{2+}$	—	3.34	3.38	3.42	3.45					
μ_{tot} $Fe1^{3+}$	4.15	3.96	4.03	4.08	4.14	3.90[a]	3.86	3.91	3.96	4.01
μ_{tot} $Fe2^{2+}$	3.65	3.44	3.49	3.54	3.56					
band gap	—	1.8	2.1	2.4	2.7	—	0.9	1.0	1.0	1.1

- magnetic moments in good agreement with exp. (**GGA+U**)
  - **whereas LDA/GGA:** CO: 3.37/3.02 VM: 3.34 μ_B
  - orbital moments small (but significant for Fe^{2+})
- band gap: smaller for VM than for CO phase (**GGA+U**)
  - exp: semiconductor (like Ge); VM phase has increased conductivity
  - **LDA/GGA:** metallic

Charge transfer

- Charges according to Baders "Atoms in Molecules" theory
  - *Define an "atom" as region within a zero flux surface* $\vec{\nabla}\rho \cdot \vec{n} = 0$
  - *Integrate charge inside this region*

	CO		VM	
Atom	Multiplicity	Charge	Multiplicity	Charge
Ba	4	+1.51	8	+1.52
Y	4	+2.17	8	+2.15
$Fe1^{3+}$	4	+1.84	16	+1.62
$Fe2^{2+}$	4	+1.36		
O1	4	−1.36	8	−1.36
O 2*a*	4	−1.40	16	−1.39
O 2*b*	4	−1.36		
O3	8	−1.38	16	−1.39

Structure optimization (GGA+U)

- CO phase:
  - *Fe^{2+}: shortest bond in y (O2b)*
  - *Fe^{3+}: shortest bond in z (O1)*
- VM phase:
  - *all Fe-O distances similar*
  - *theory deviates along z !!*
    - Fe-Fe interaction
    - different U ??
    - finite temp. ??

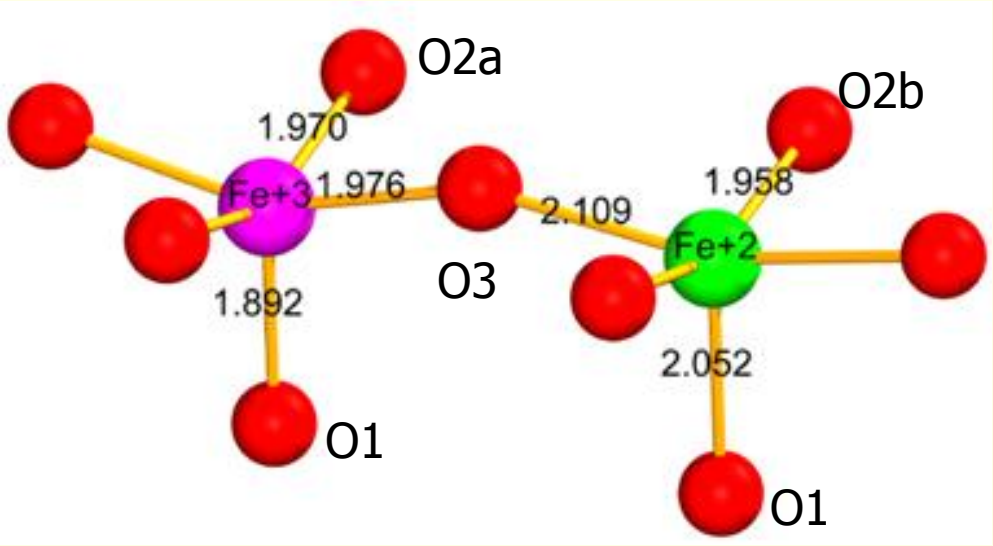

Bond	Direction	CO		VM	
		exp.	theory	exp.	theory
$Fe1^{3+}$ - O1	z	1.892	1.899	1.999	2.056
$Fe2^{2+}$ - O1		2.052	2.057		
$Fe1^{3+}$ - O2b	y	1.970	1.968	1.995	1.983
$Fe2^{2+}$ - O2a		1.958	1.965		
$Fe1^{3+}$ - O3	x	1.976	1.957	2.000	1.989
$Fe2^{2+}$ - O3		2.109	2.128		
$Fe1^{3+}$ - $Fe2^{2+}$	z	3.587	3.576	3.571	3.456

Can we understand these changes ?

- **Fe^{2+} ($3d^6$)** **CO** **Fe^{3+} ($3d^5$)** **VM** **$Fe^{2.5+}$ ($3d^{5.5}$)**
- **majority-spin fully occupied**
- strong covalency effects in e_g and d-xz orbitals
- very localized states at lower energy than Fe^{2+}
- **minority-spin states**
- d-xz fully occupied (localized)
- empty
- $d\text{-}z^2$ partly occupied
- ⇨ short bond in y
- short bond in z (one O missing)
- FM Fe-Fe; distances in z ??

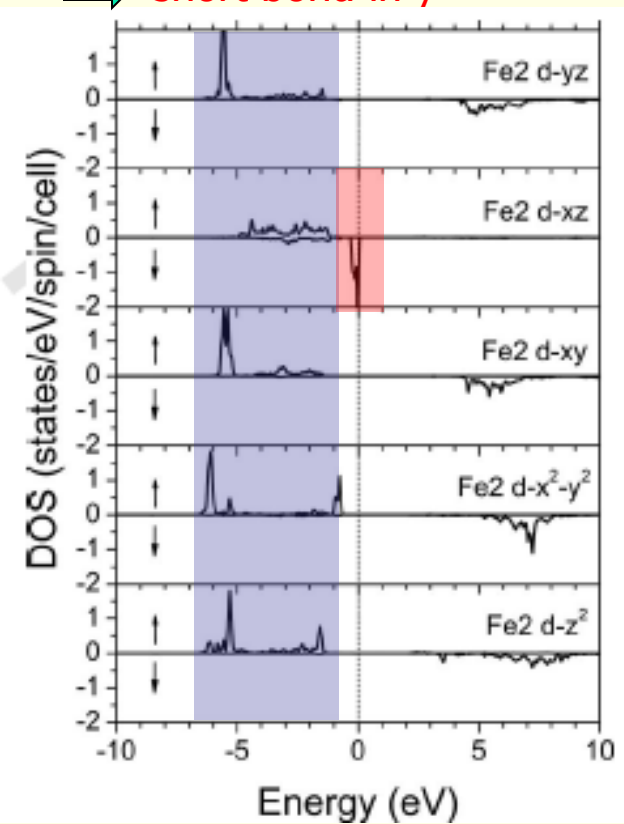

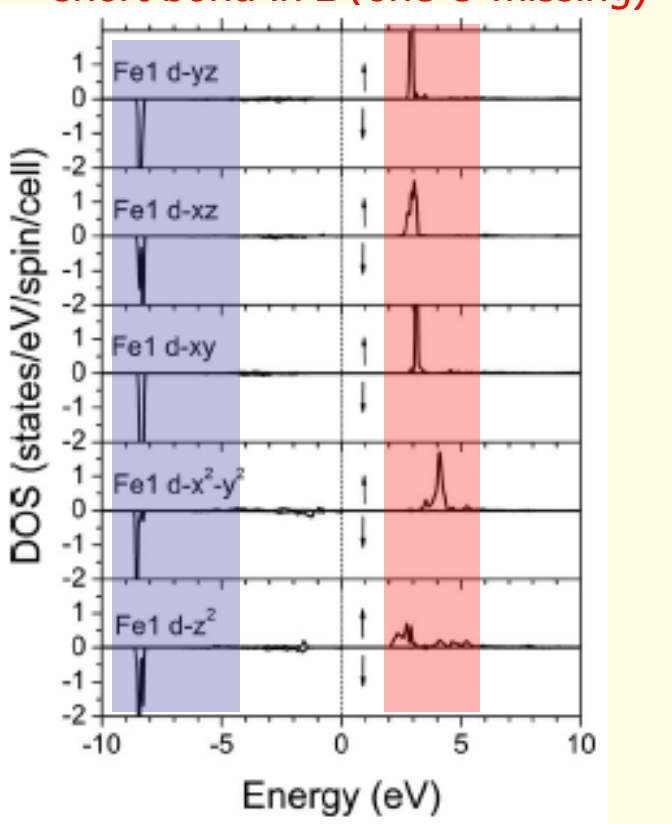

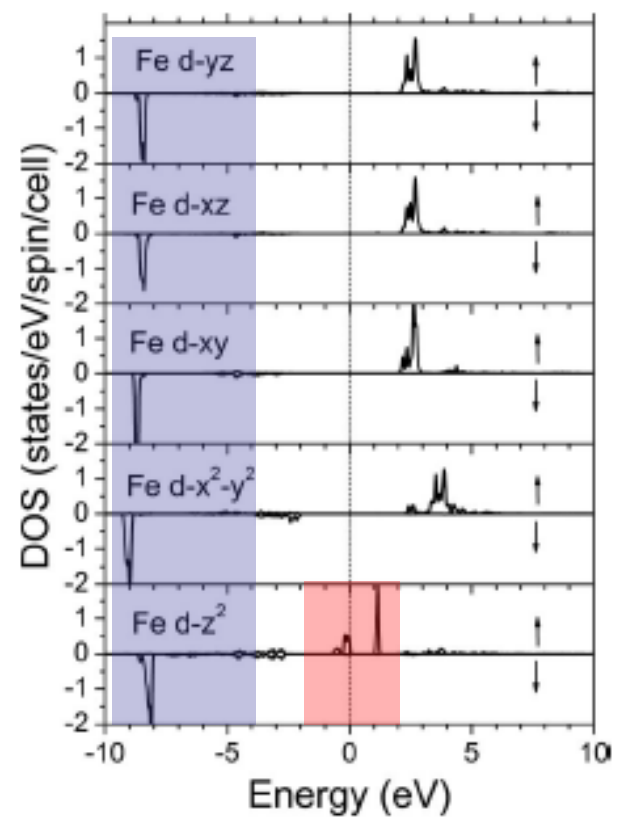

Difference densities $\Delta\rho=\rho_{cryst}-\rho_{at}^{sup}$

- CO phase

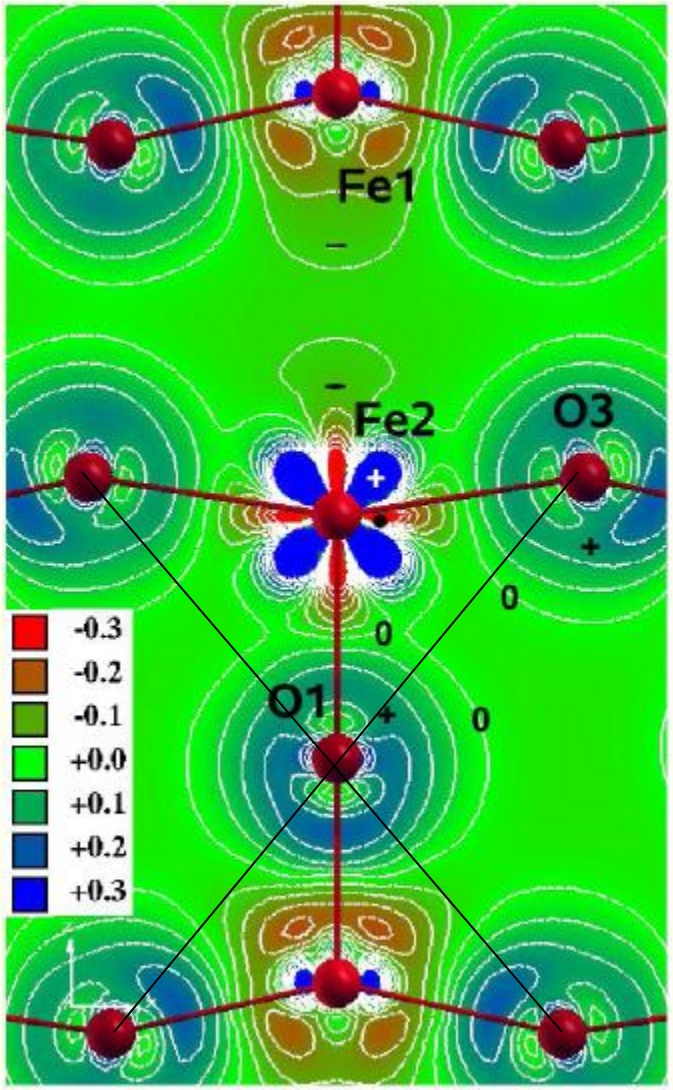

Fe1 Fe^{3+}: d-x^2
Fe2 Fe^{2+}: d-xz
O1 and O3: polarized toward Fe^{3+}

Fe: d-z^2 Fe-Fe interaction
O: symmetric

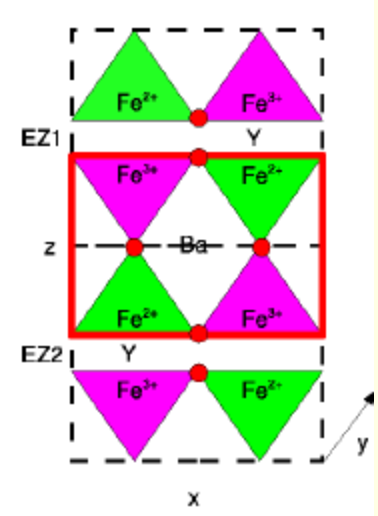

VM phase

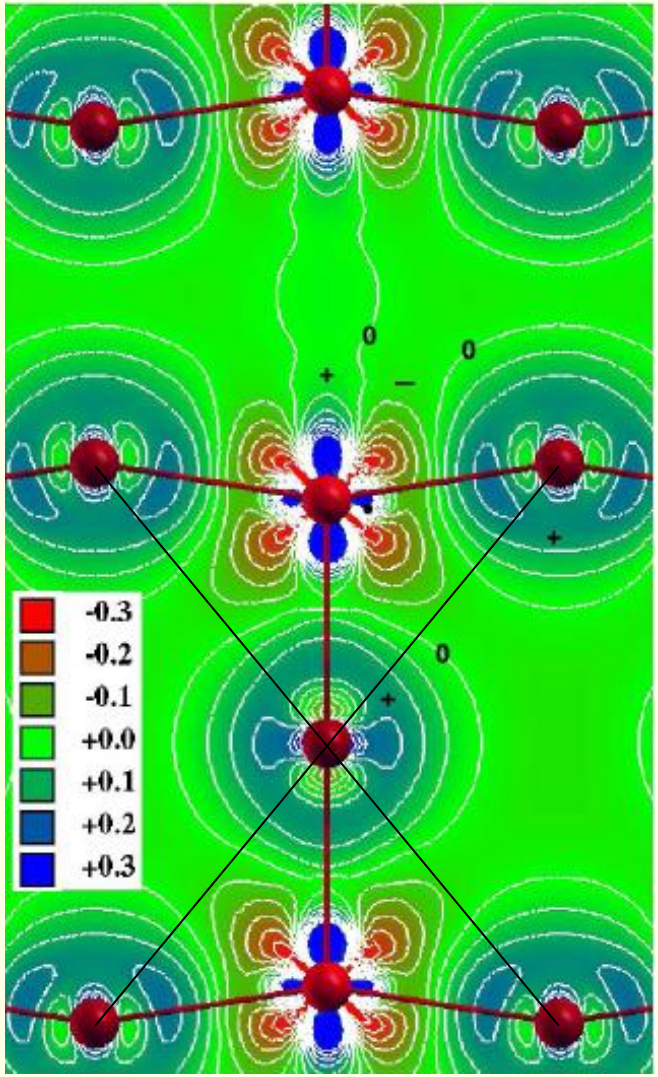

d_{xz} spin density (ρ_{up}-ρ_{dn}) of CO phase

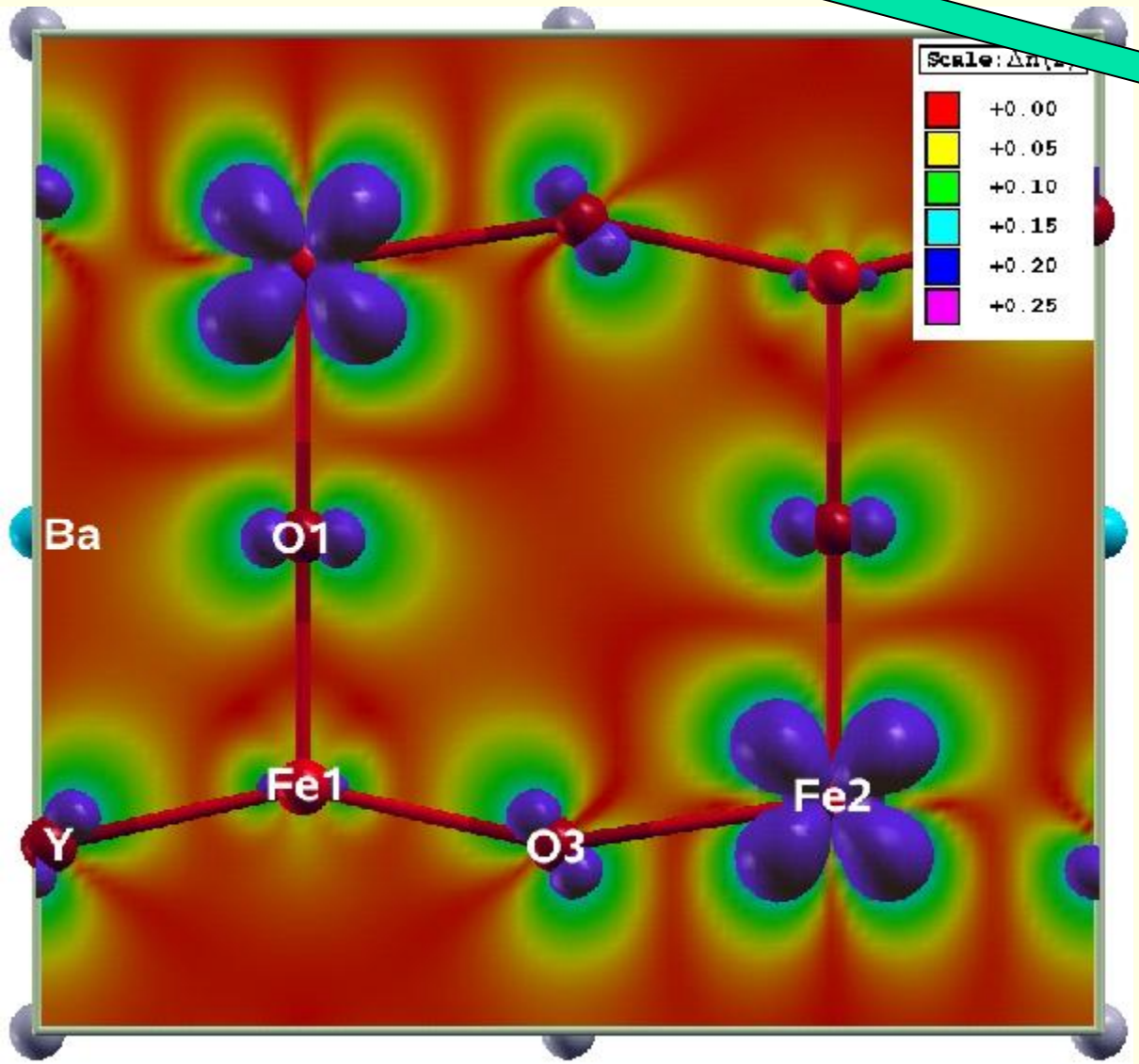

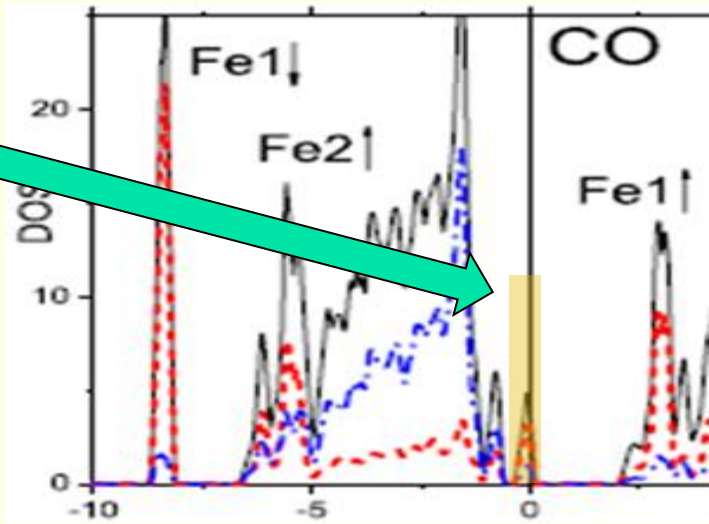

Fe^{3+}:(Fe1) no contribution

Fe^{2+}:(Fe2) d_{xz}

weak π-bond with

O tilting of O3 π-orbital

EFG: Fe^{2+} has too small anisotropy in LDA/GGA

TABLE VIII: Hyperfine fields B (in Tesla), isomer shifts δ (mm/s) and quadrupole coupling constants eQV_{zz} (mm/s) for the CO phase for various exchange and correlation potentials and experiment[8–10].

CO

		exp.	GGA+U				LDA	GGA
	U_{eff} [eV]	—	5	6	7	8	—	—
$Fe2^{2+}$	B_{dip}	—	-16.29	-16.49	-16.66	-16.83	-6.68	-12.67
	B_{orb}	—	-6.73	-6.90	-8.26	-7.65	-9.57	-6.34
	$B_{contact}$	—	32.25	32.23	32.58	32.60	32.21	31.58
	B_{tot}	~ 8	9.23	8.83	7.66	8.13	15.96	12.57
	δ	~ 1	0.92	0.94	0.96	0.99	0.74	0.79
	eQV_{zz}	3.6 – 4[a]	3.66	3.74	3.81	3.89	-0.82	2.60
$Fe1^{3+}$	B_{dip}	—	-0.67	-0.60	-0.52	-0.45	1.29	0.39
	B_{orb}	—	-0.52	-0.45	-0.37	-0.28	-7.96	-2.65
	$B_{contact}$	—	37.65	38.28	38.15	37.86	29.64	31.63
	B_{tot}	~ 50	36.46	37.24	37.26	37.12	22.97	29.37
	δ	~ 0.4	0.33	0.30	0.28	0.25	0.50	0.47
	eQV_{zz}	1 – 1.5[a]	1.46	1.50	1.51	1.52	1.04	-0.30

[a]depending on rare earth ion

VM

		exp.	GGA+U				LDA	GGA
	U_{eff} [eV]	—	5	6	7	8	—	—
$Fe^{2.5+}$	B_{dip}	—	-3.00	-2.98	-2.95	-2.87	-2.13	-2.83
	B_{orb}	—	-3.11	-2.99	-2.84	-2.74	-5.47	-4.56
	$B_{contact}$	—	41.17	40.96	41.45	41.17	33.10	36.36
	B_{tot}	~ 30	35.06	34.98	35.67	35.56	25.50	28.98
	δ	~ 0.5	0.53	0.52	0.51	0.49	0.60	0.60
	eQV_{zz}	~ 0.1	0.12	0.13	0.13	0.13	0.19	-0.27

magnetic interactions

- CO phase:
  - *magneto-crystalline anisotropy:*
    moments point into y-direction
    in agreement with exp.

direction [hkl]	energy [Ry]
[100]	-115.578,24026
[010]	-115.578,24065
[001]	-115.578,24024

  - *experimental G-type AFM structure (AFM direct Fe-Fe exchange) is 8.6 meV/f.u. more stable than the magnetic VM phase (direct FM)*

- VM phase:
  - *experimental "FM across Y-layer"*
    AFM structure (FM direct Fe-Fe exchange) is 24 meV/f.u. more stable than magnetic order of CO phase (G-type AFM)

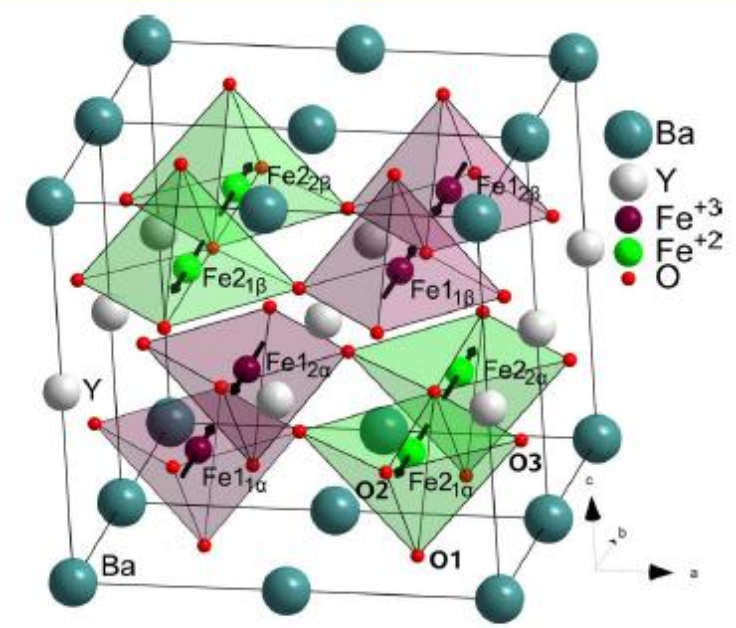

FIG. 1. (Color online) The magnetic 1×2×1 CO supercell. The arrows depict the direction of the magnetic moments.

Verwey transition in $YBaFe_2O_5$

- Standard LDA/GGA methods cannot explain $YBaFe_2O_5$
  - *metallic, no charge order (Fe^{2+}-Fe^{3+}), too small moments*
- Needs proper description of the Fe 3d electrons (GGA+U, …)
- CO-phase: Fe^{2+}: high-spin d^6, occupation of a single spin-dn orbital (d_{xz})
  - *Fe^{2+}/Fe^{3+} ordered in chains along b,*
  - *cooperative Jahn-Teller distortion and strong e^--lattice coupling*
- VM phase: small orthorhombic distortion (AFM order, moments along b)
  - *Fe d-z^2 spin-down orbital partly occupied (top of the valence bands)*
  - *leads to direct Fe-Fe exchange across Y-layer*
  - *and thus to ferromagnetic order (AFM in CO phase).*
- Quantitative interpretation of the Mössbauer data

C.Spiel, P.Blaha, K.Schwarz, Phys.Rev.B.79, 085104 (2009)

2. example: Hexagonal-Boronnitride on TM-surfaces

Decomposition of **borazin**
on hot **transition metal surfaces**
2 representative cases:

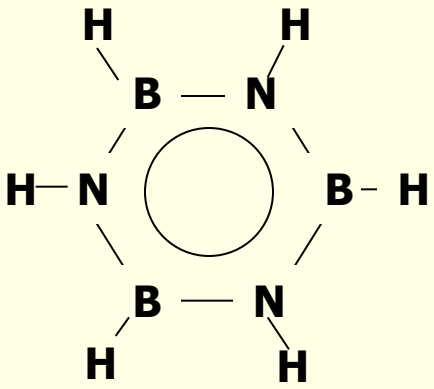

i) **h-BN / Ni(111): simple monolayer**

ii) **h-BN / Rh(111): "nanomesh" with**
12x12 Rh(111) superstructure
(Greber+Osterwalder, Uni Zürich)

Why different ?

	8	9	10	11
3d	Fe	Co	**Ni**	Cu
4d	Ru	**Rh**	Pd	Ag
5d	Os	Ir	Pt	Au

h-BN on transition metal-surfaces

- thermal decomposition of borazine $(HBNH)_3$ on hot TM metal surfaces (~1000K)
- forms simple (1x1) or very complex structures -

borazine $(HBNH)_3$

as seen by STM

- h-BN/**Ni**(111) 0.25 nm
- h-BN/**Rh**(111) 3.2 nm

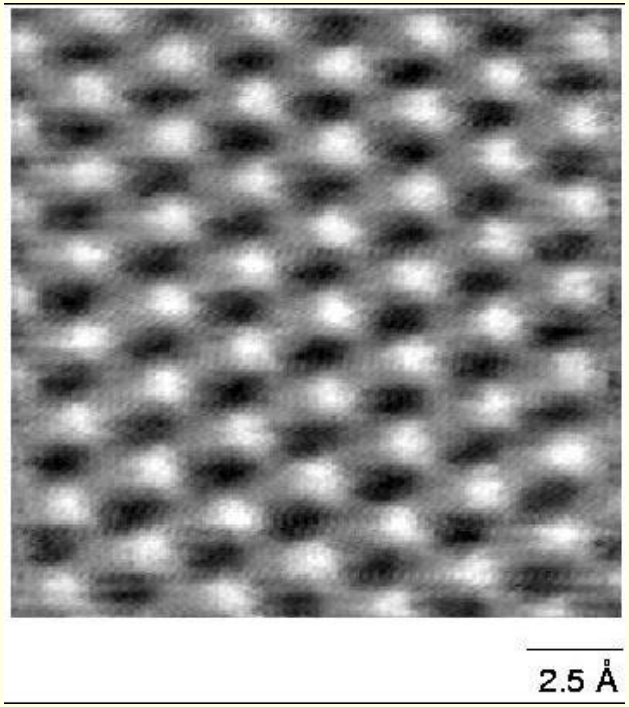

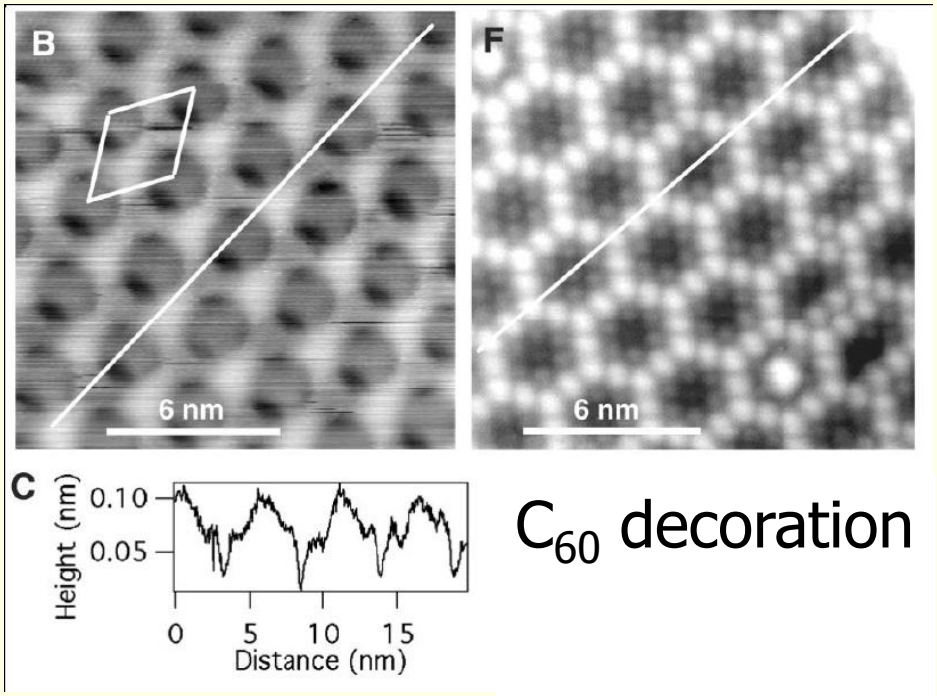

C_{60} decoration

Strain energy of BN on TM(111)

Lattice mismatch

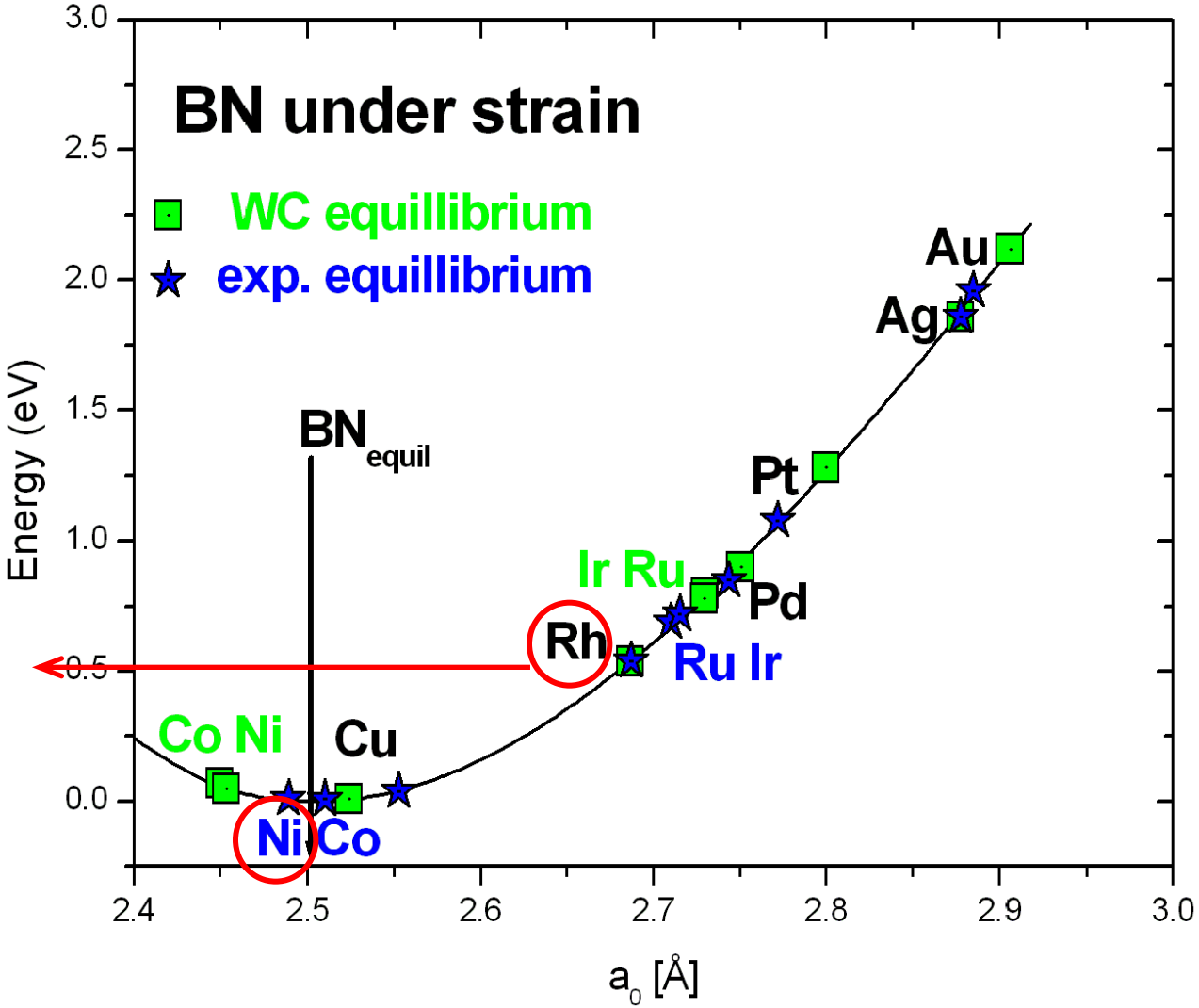

0.5eV/BN

Geometric structure of h-BN/Ni(111)

- **G.Grad, P.Blaha, K.Schwarz W.Auwärter, T.Greber,** Phys.Rev. B **68**, 085404 (2003)
- Hexagonal boronnitride grown epitaxially on a Ni(111) surface
- Modelling of the h-BN/Ni(111) interface by a slab-supercell
- fcc Ni has (ABCABC…) stacking
- N and B atoms can occupy „top", „hcp" or „fcc" sites

- N occupies the „top" site
- „buckling" of BN:
  - exp. 2.04/2.19 (0.07) Å
  - theory 2.09/2.19 (0.10) Å
- BN-layer spacing in pure h-BN: 3.33 Å

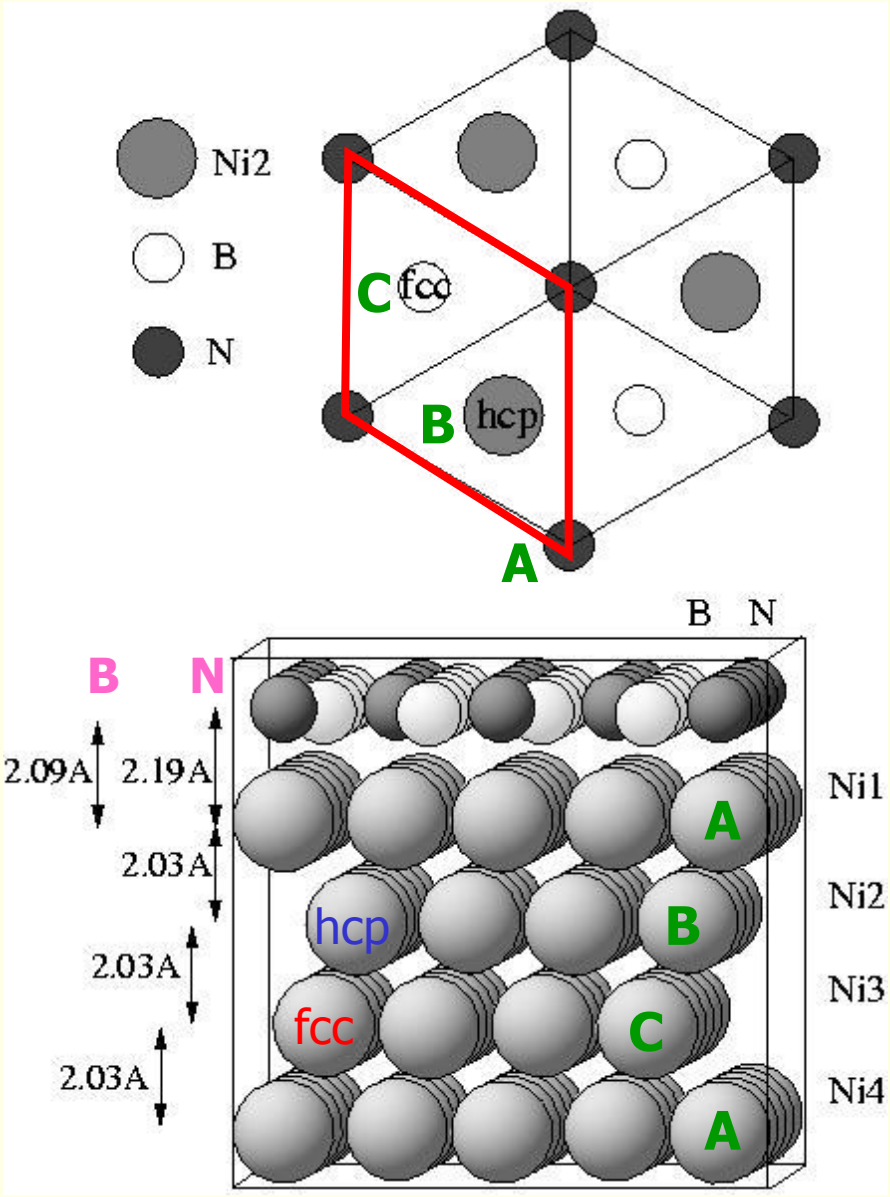

Theoretical Method

WIEN2k (APW+lo method)

- DFT simulation
- Surface simulated with 3-d periodic system

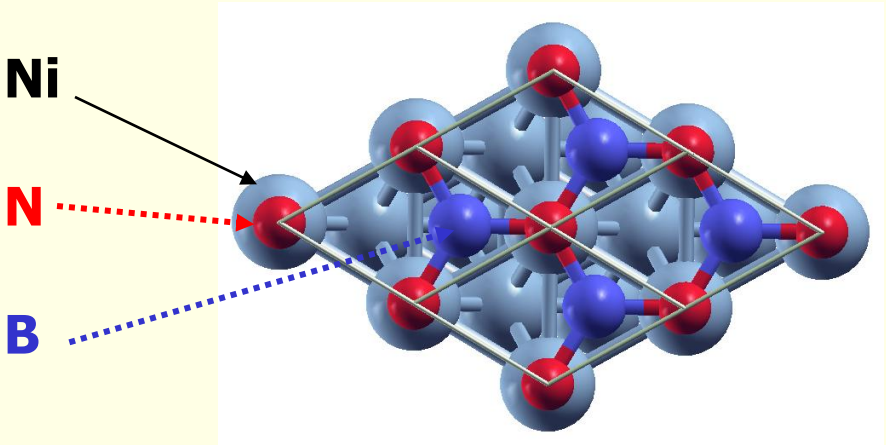

BN

7 layer-Ni

BN

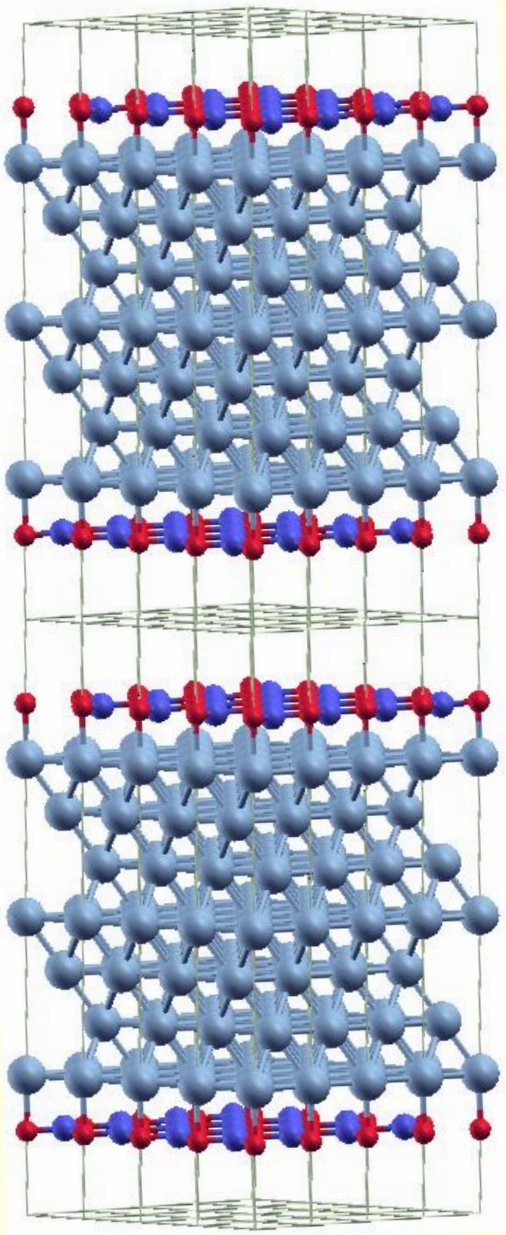

Possible positions of B and N on Ni(111):

- Only N on „top" of Ni gives stable structures
- (top,fcc) by only 9 meV/BN more stable than (top,hcp)

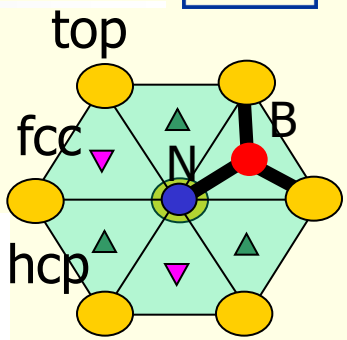

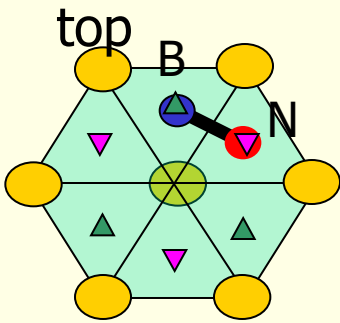

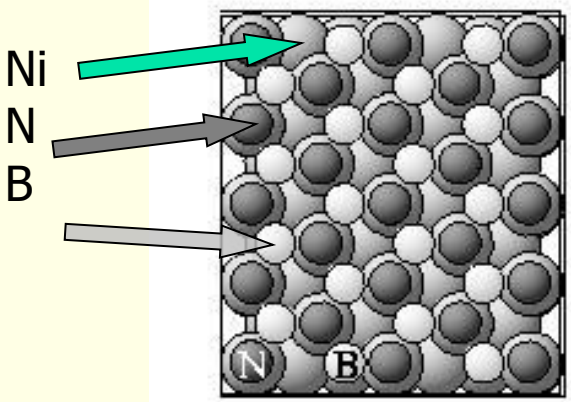

(N,B)=(top,fcc)

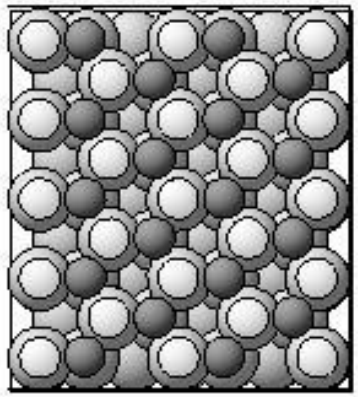

(N,B)=(hcp,top)

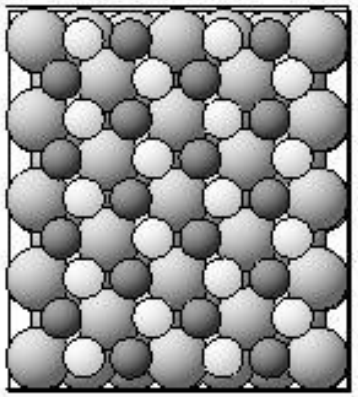

(N,B)=(fcc,hcp)

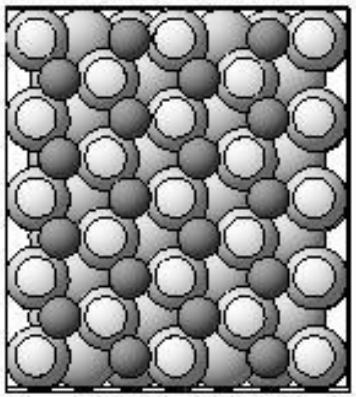

(N,B)=(fcc,top)

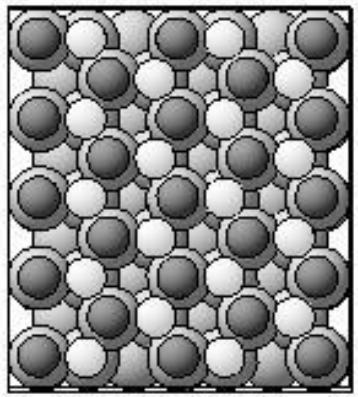

(N,B)=(top,hcp)

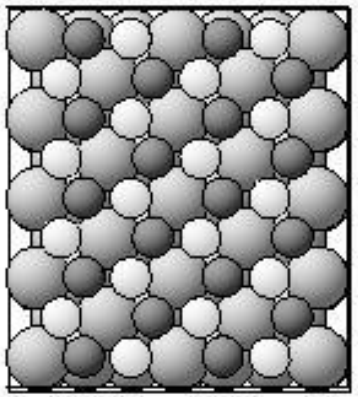

(N,B)=(hcp,fcc)

STM-data of h-BN/Ni(111)

$$I_t \propto \sum_v |\Psi_v(r_0)|^2 \delta(E_v - E_F)$$

Electron densities at
E_F +/- 0.08eV
r_0: 2.5 Å from surface

- Exp: three different sites are visible. Which site is dark? Which white ?

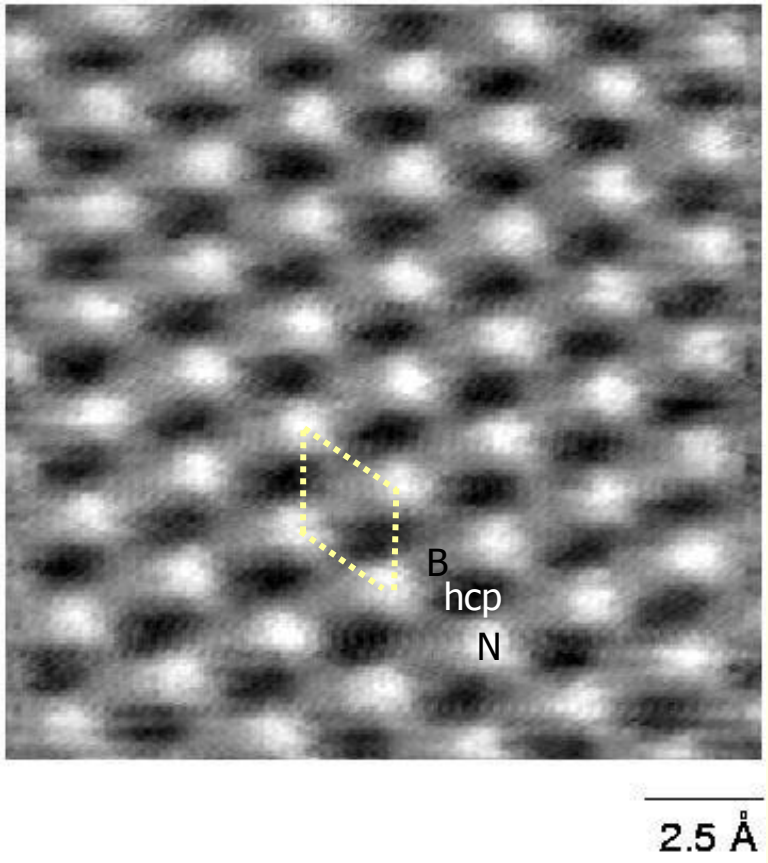

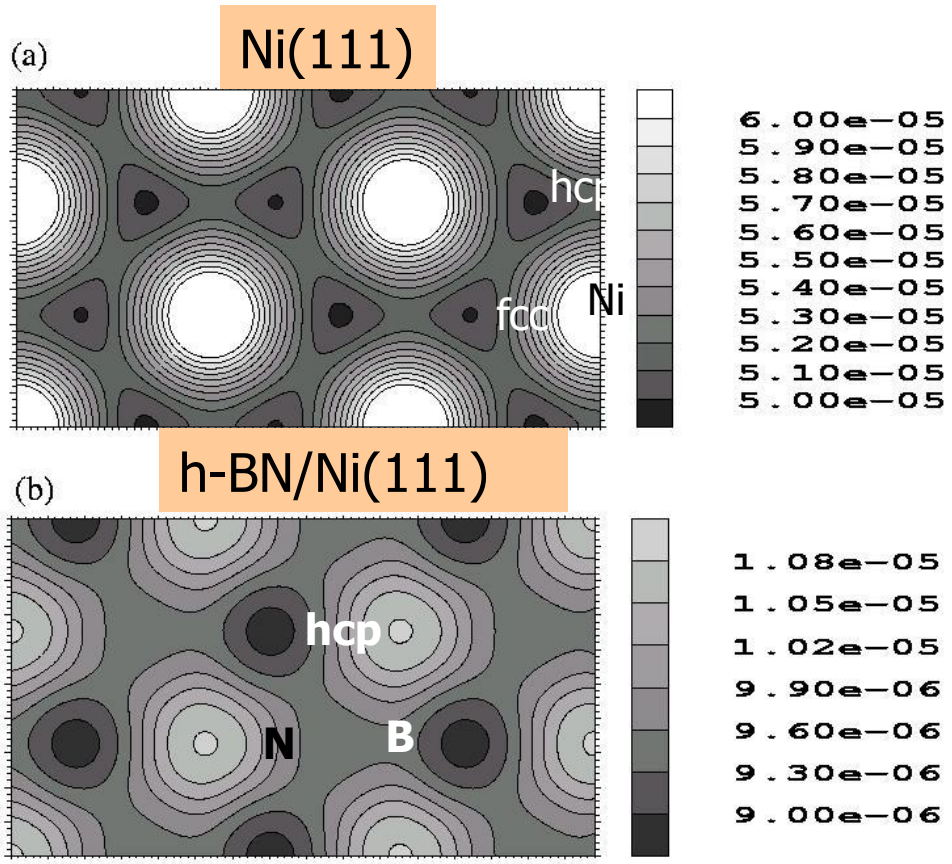

Work function

W (001) surface

Work function

potential

supercell

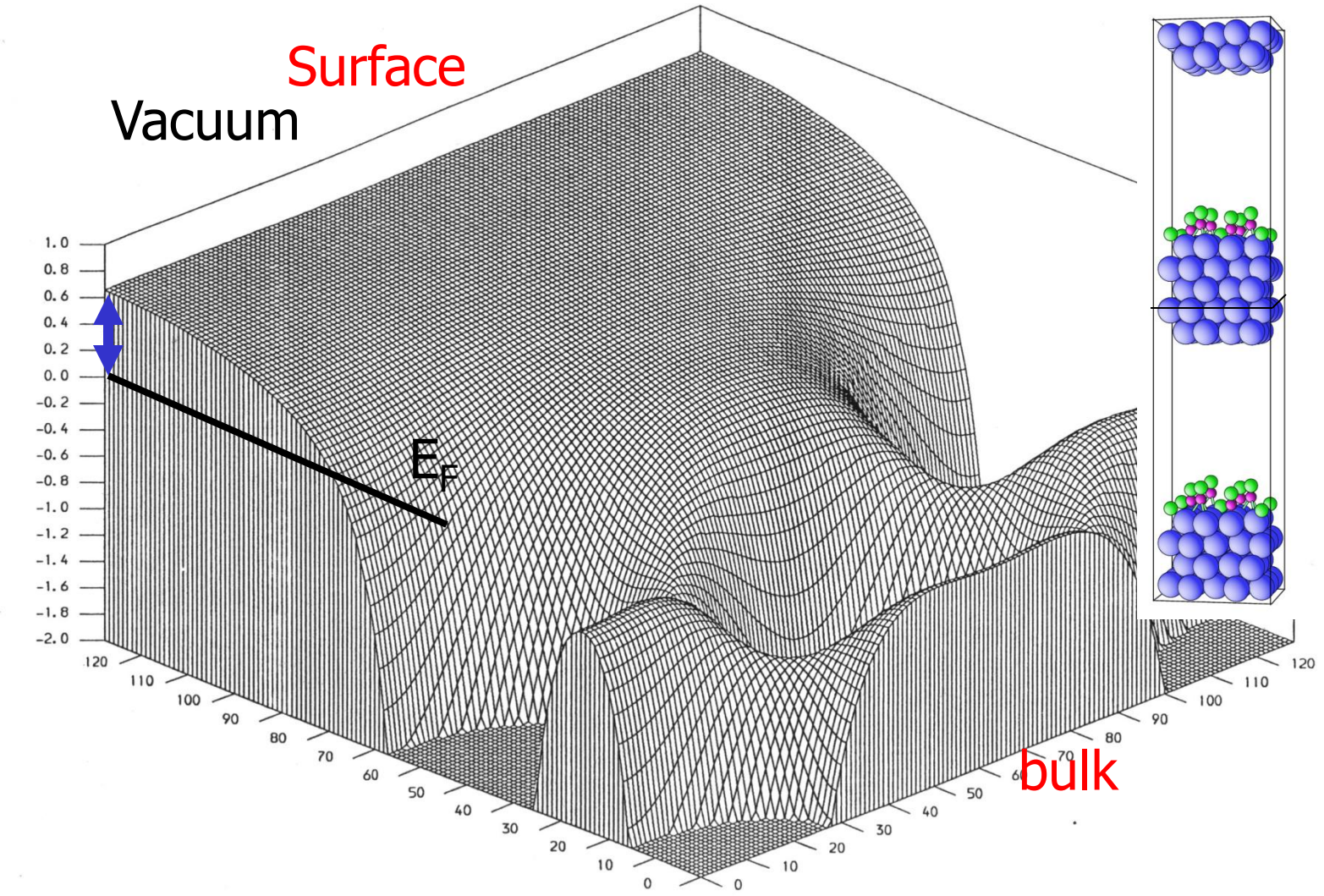

Workfunction shift:

workfunction:

Ni	h-BN/Ni	
5.3	3.5 eV	exp.
5.6	3.9 eV	theory

charge transfer
(Bader's AIM method):

	N	B	Ni
free h-BN-l:	-0.56	+0.56	e⁻
h-BN/Ni:	-0.59	+0.65	-0.06

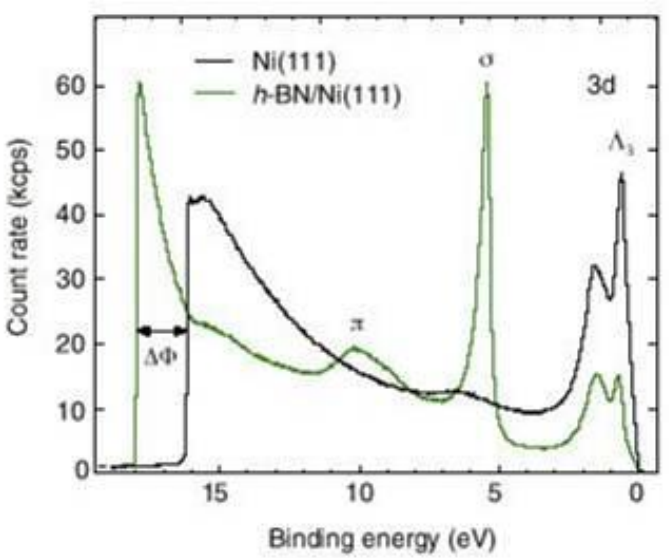

FIG. 2. He I normal emission UP-spectra for Ni(111) and *h*-BN/Ni(111). The work function decrease and the shift of the Λ_1 Ni *d* band feature upon formation of the the *h*-BN layer indicate a decrease of the Ni magnetic moment (for details see text).

Intensity drop!

electrostatic picture with 1 Å charge separation➔ 2eV shift

additional 0.06e should fill Ni-dn states: ➔ smaller moment

Magnetic moments (19 Ni-layers):

- pure Ni(111) surface:
  - *surface moments enlarged (localization)*
  - *Friedel oszillations*
  - *„Bulk" value reached*
- h-BN/Ni(111) surface:
  - *surface moments reduced due to charge transfer from B to Ni-dn*
  - *Friedel oszillations*
  - *„bulk" value not reached*

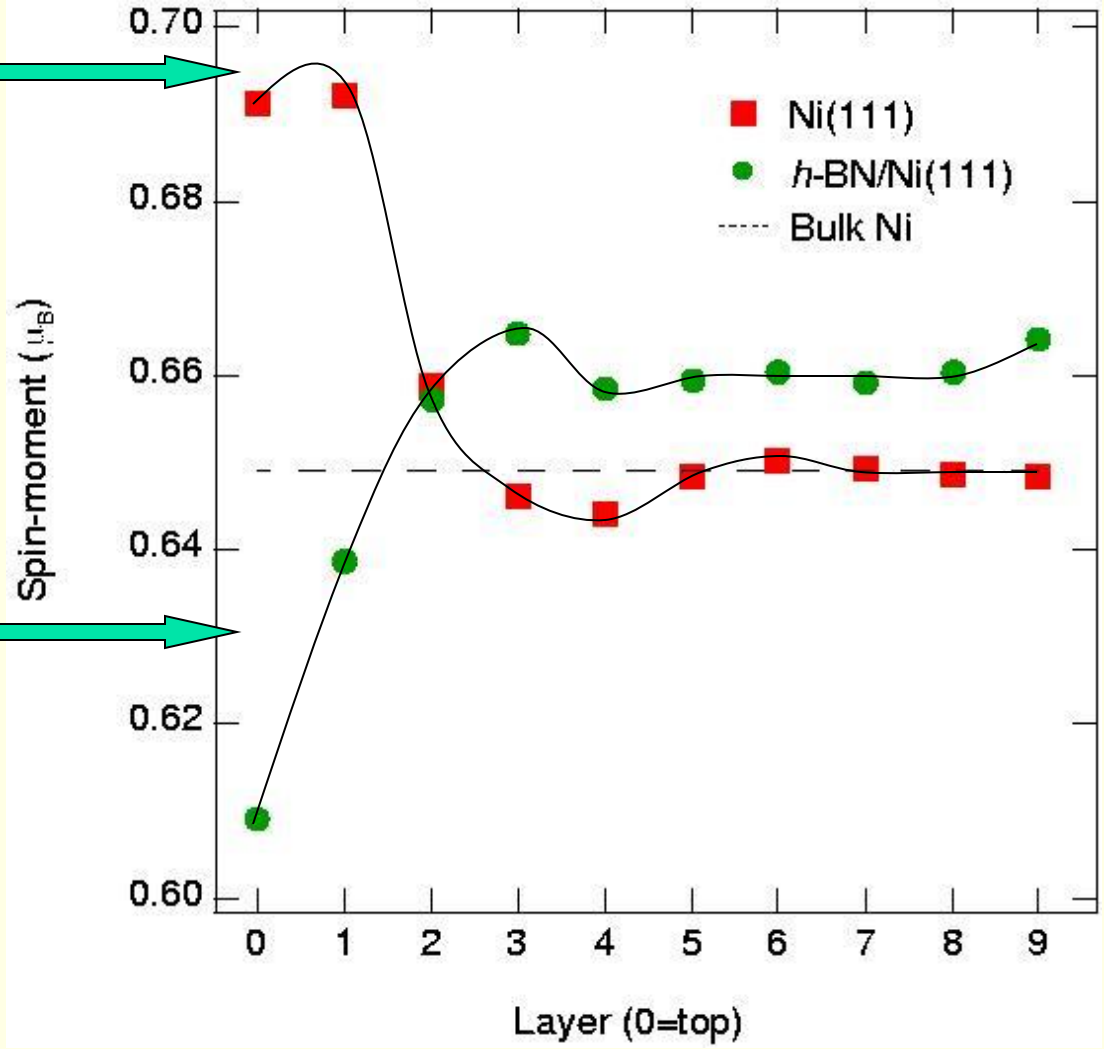

XAS: X-ray absorption spectra

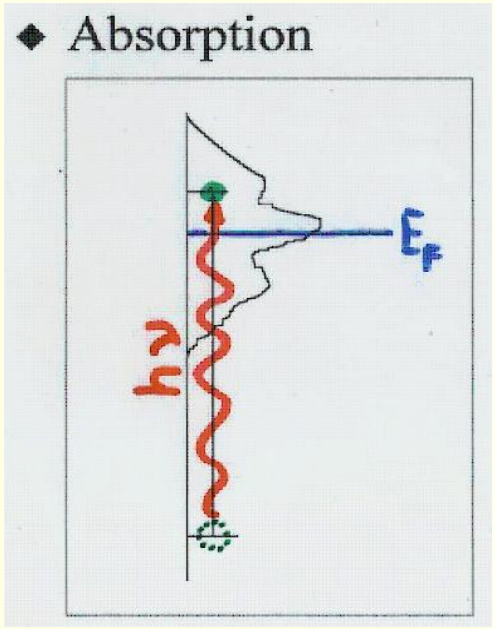

dipole operator

$$I \propto \nu^3 \left|\langle \Psi_{val} \left| r \right| \Psi_{core} \rangle\right|^2 \chi_l^A(\epsilon)$$

ℓ-like PDOS (atom A)

$$\frac{I_{n'l'}}{\nu^3} = \sum_l W_{ll'} M_A^2(l, n'l', \epsilon) \chi_l^A(\epsilon) \delta(\epsilon - E_{core}, h\nu)$$

energy conservation

$\Delta\ell = \pm 1$

dipole-section rule

Radial transition probability:

- from a core state with q.n. n´ℓ´on atom A
- to an ℓ-like conduction band state inside the atomic sphere A
- within the dipole approximation

Final state effects:
supercell with (partial) core hole on one of the atoms

Angle dependency of B-K edge in h-BN/Ni(111)

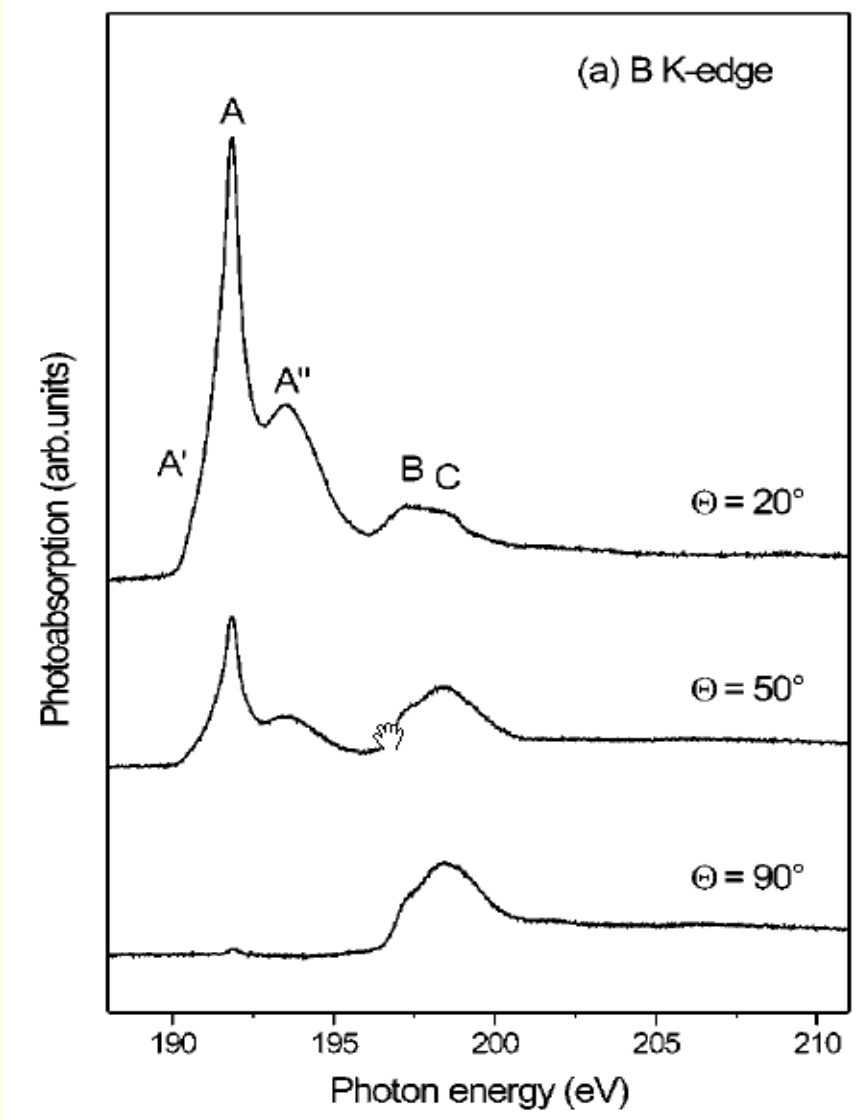

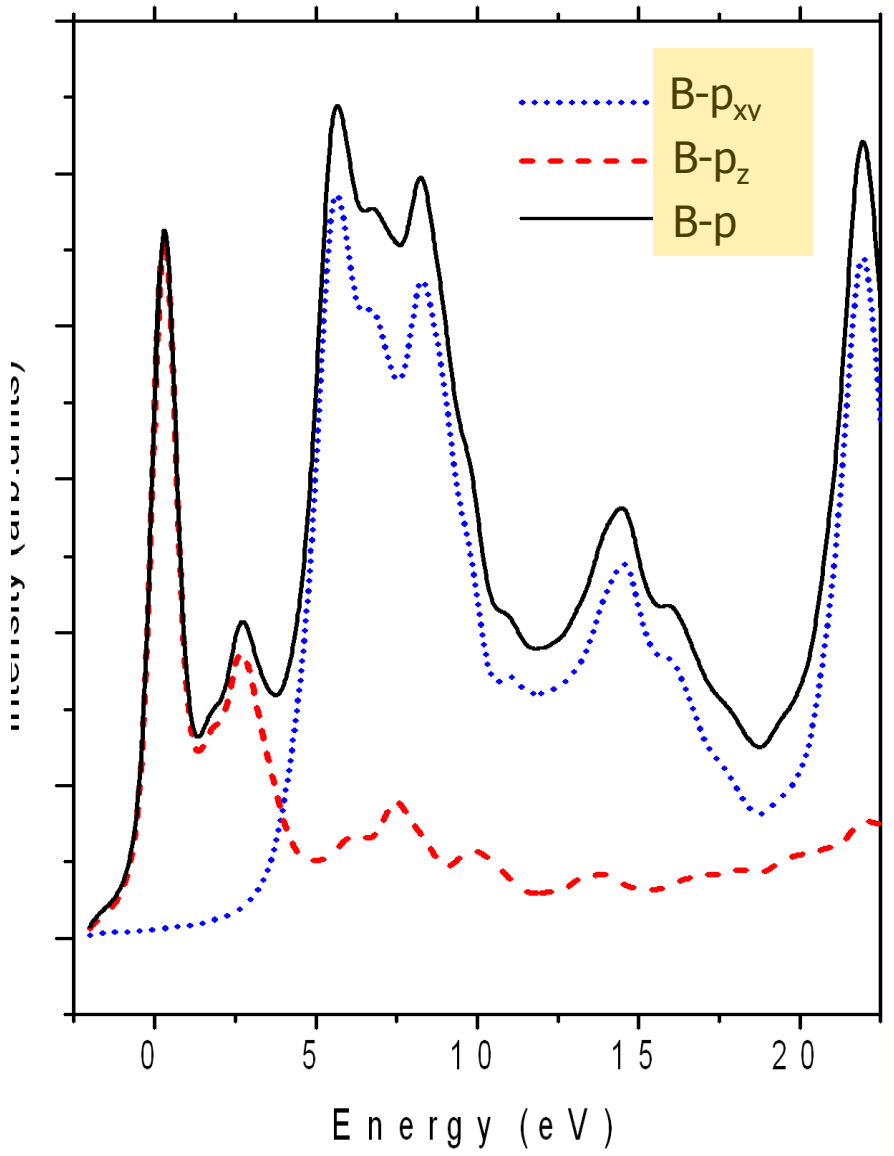

Boron nitride on **Rh**(111)

h-BN on Rh(111)

STM

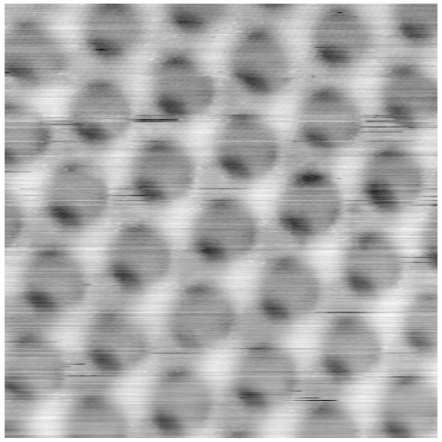

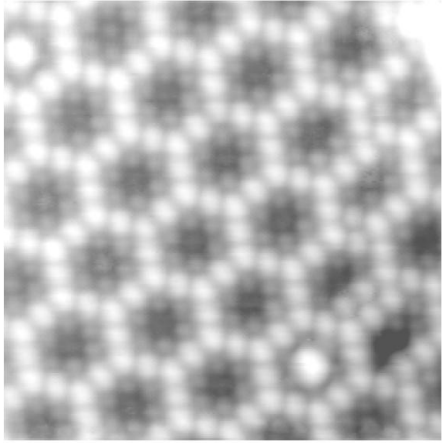

covered with C60

"lattice mismatch leads to two incomplete BN layers which form a nanomesh"

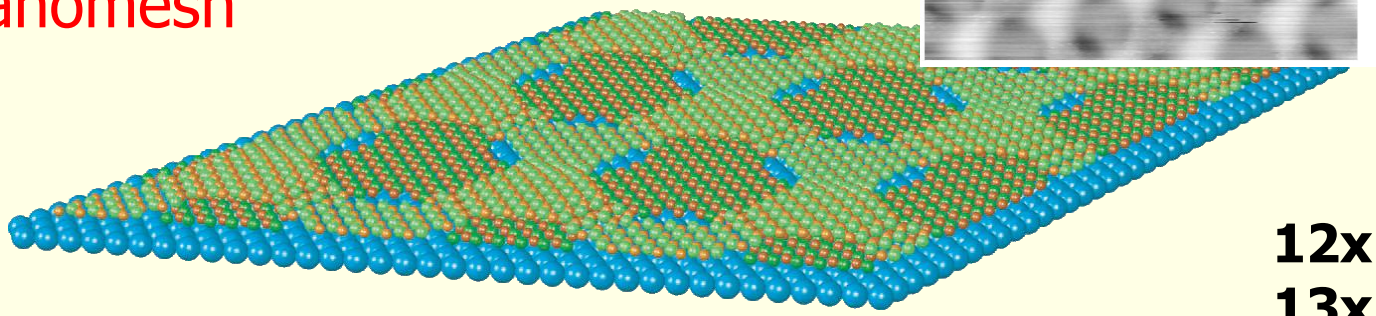

12x12 Rh
13x13 h-BN

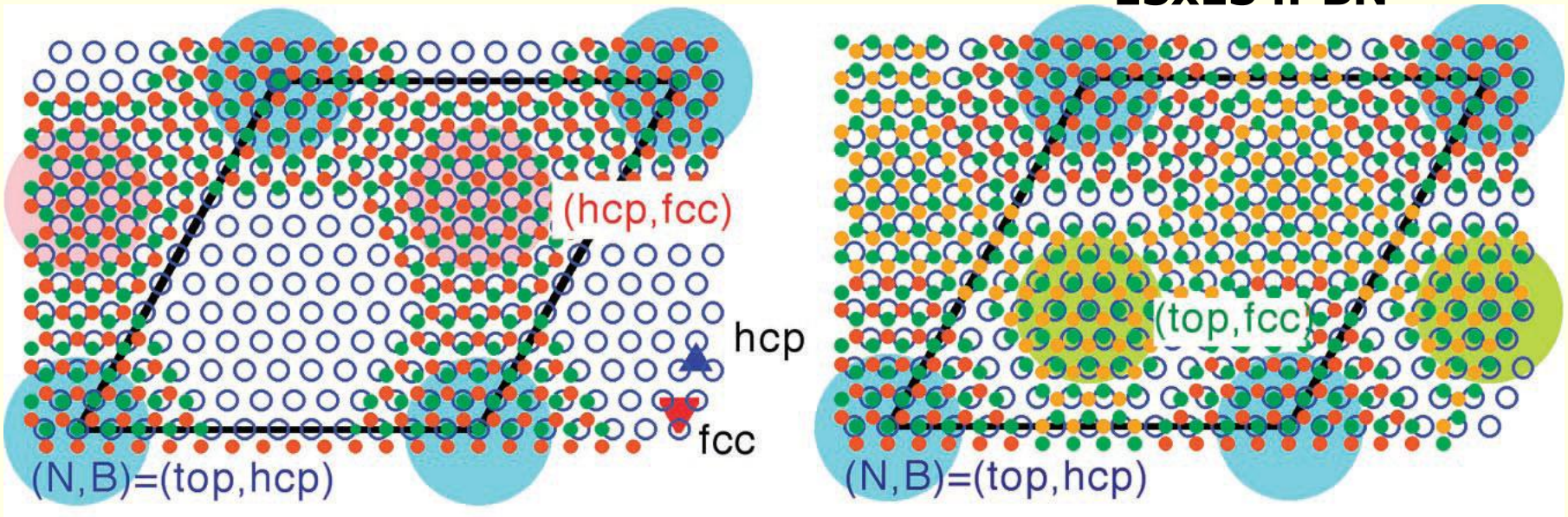

M.Corso, W.Auwärter, M.Muntwiller, A.Tamai, T.Greber:
Science, 303, 217 (2004)

Relative position of BN w.r.t. Rh(111)

A typical atomic configuration

Lattice mismatch:
13 x 13 BN
12 x 12 Rh

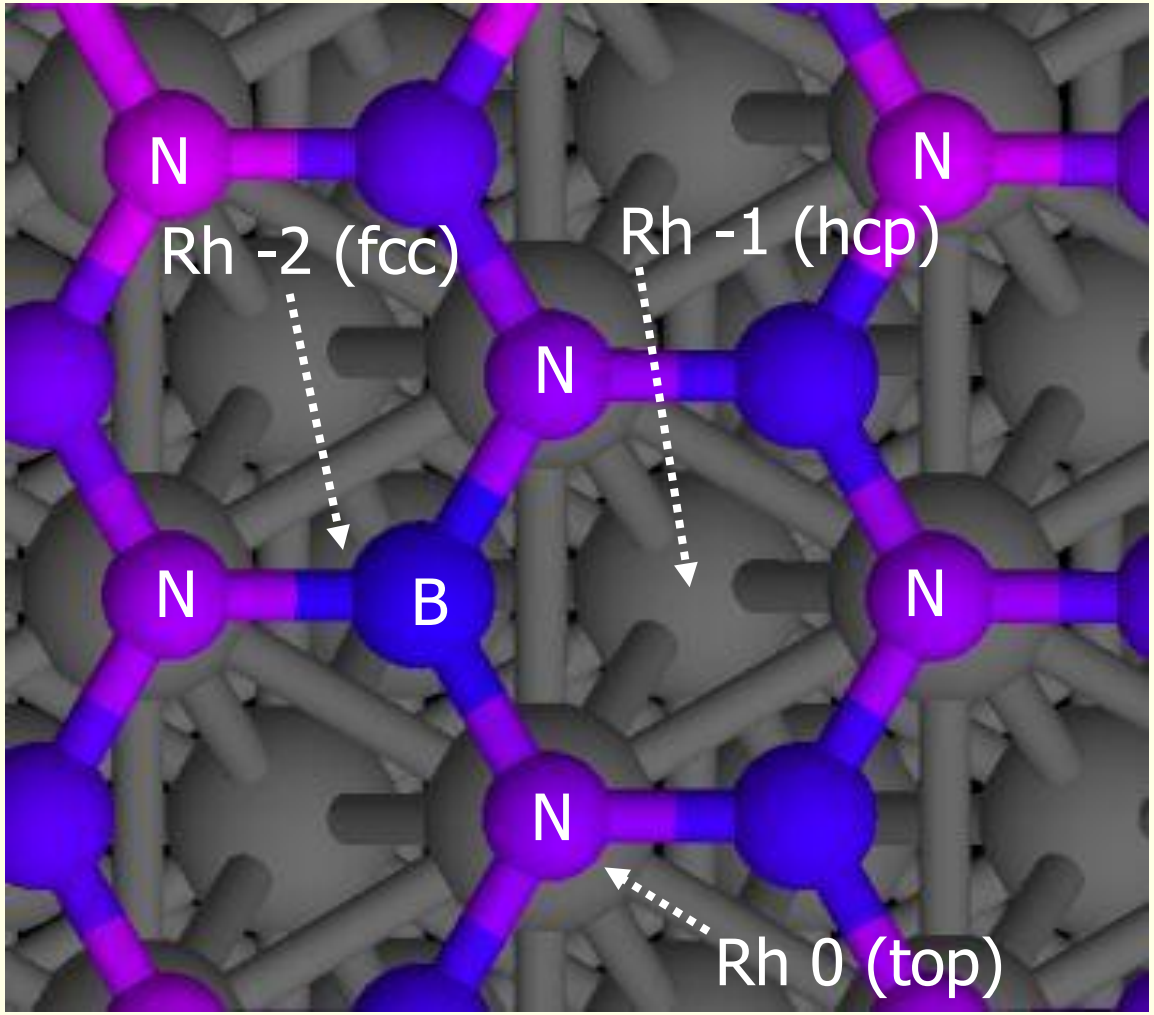

What binds BN to Rh ?

- BN at (fcc,top) position:
  - *repulsive N-forces*
  - *attractive B forces dominate*

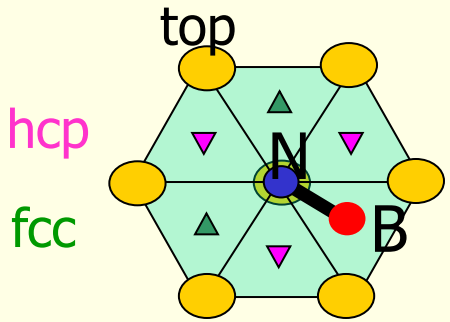

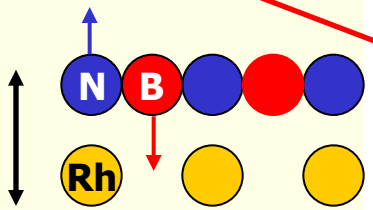

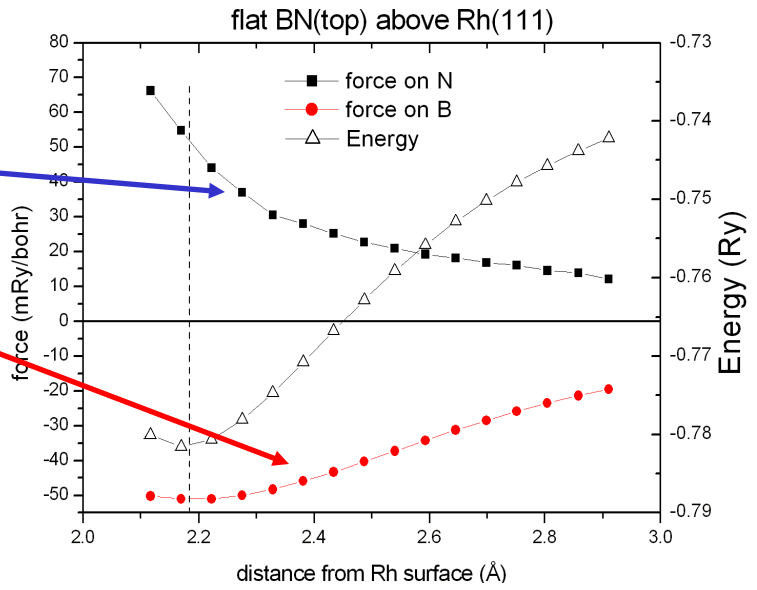

- BN at (hcp,fcc) position:
  - *repulsive N-forces dominate attractive B-forces*

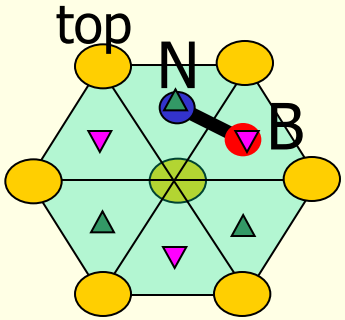

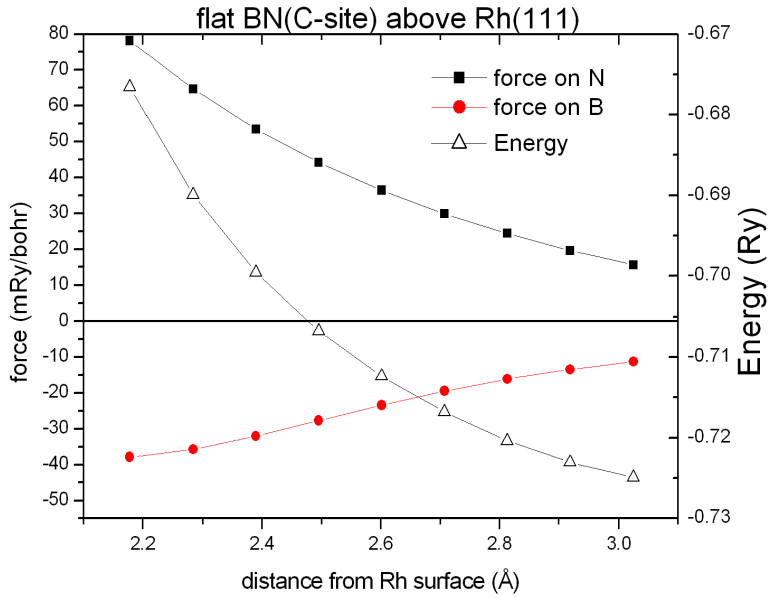

Rh – B, N interactions

Rh-B antibonding state above E_F

Rh-N antibonding state below E_F

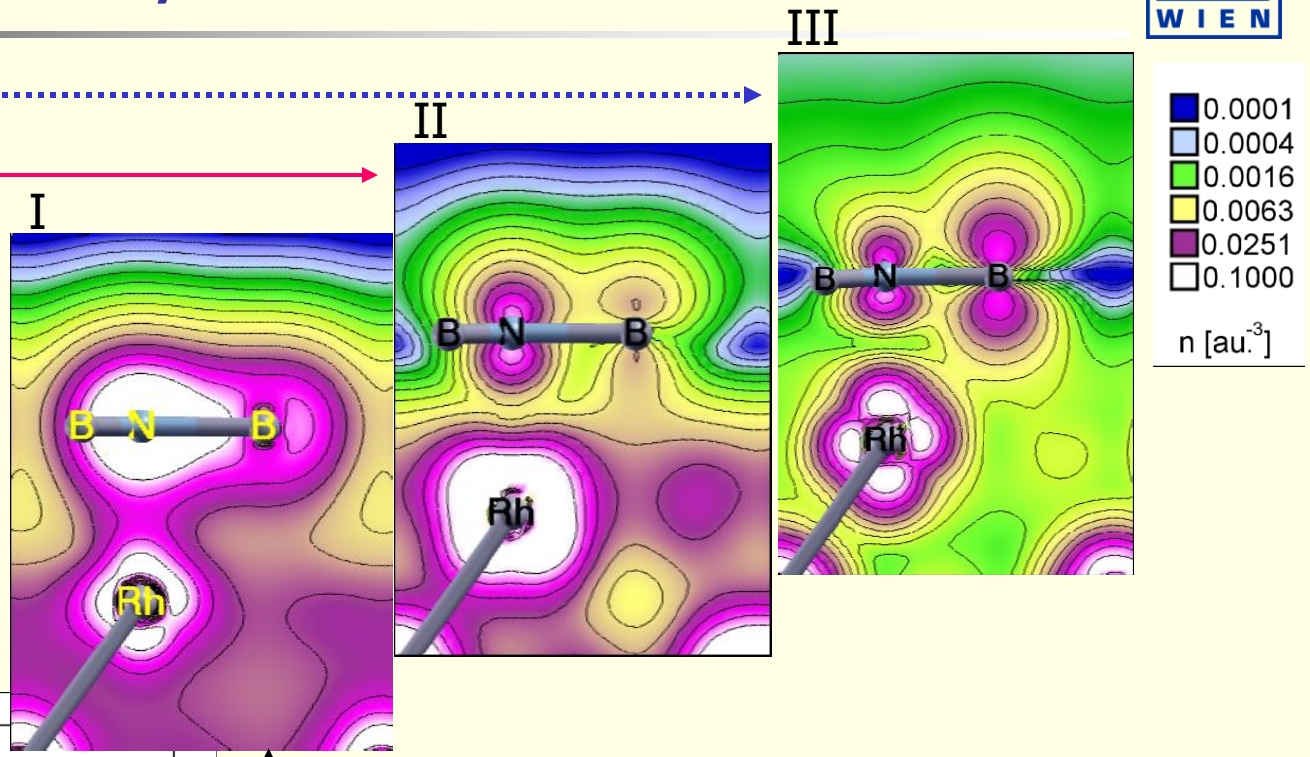

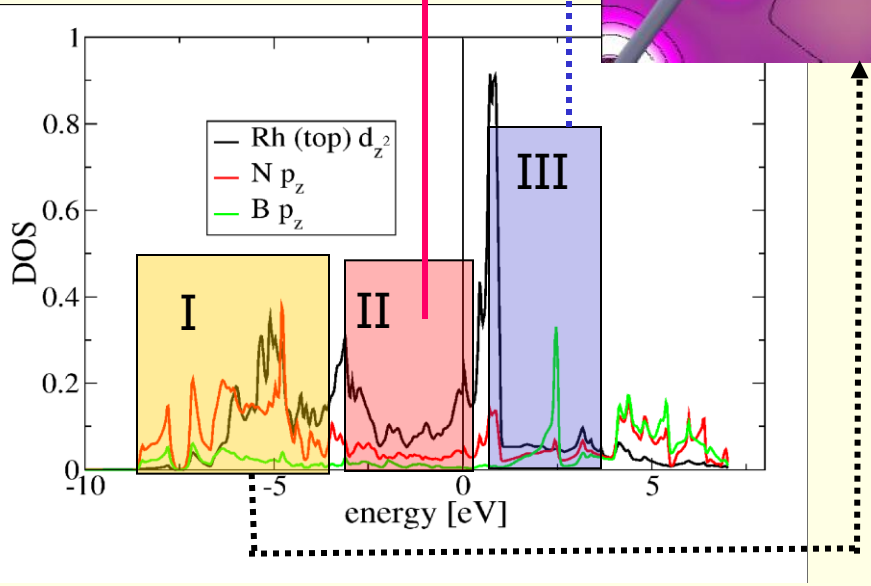

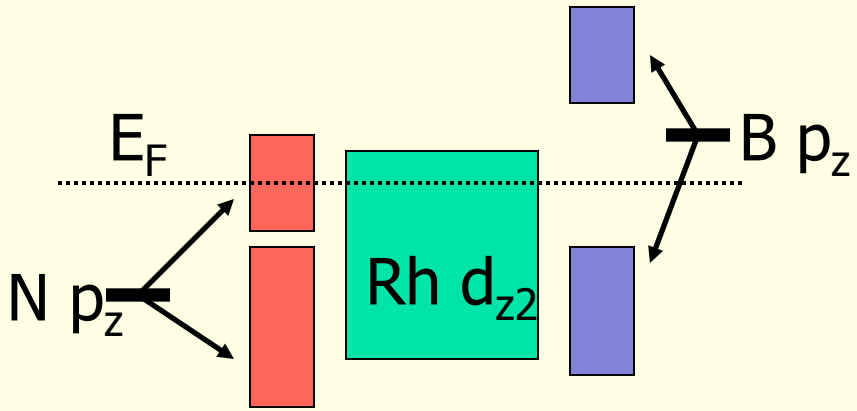

schematic bonding diagram

Force field for h-BN/Rh(111)

- separate BN-Rh from B-N interaction
- freeze Rh underlayer

Rh(111)-N,B interaction

ab-initio calculated force field

$F_{N,B} = F_{N,B}(x,y,z)$

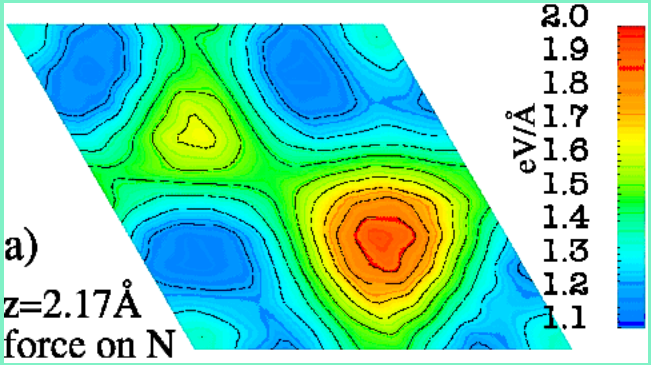

- stretched h-BN in 1x1 geometry
- stretching has minor influence on forces

elastic h-BN

restoring force, elastic model

$$F_r = k_s.d_s + k_b.d_b$$

response to stretching and buckling deformations

12x12 Rh supercell
13x13 h-BN supercell
geometry optimization

Single h-BN layer on Rh(111)

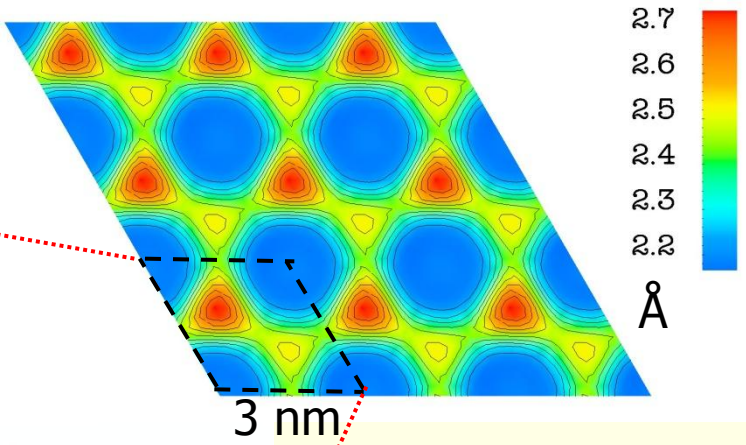

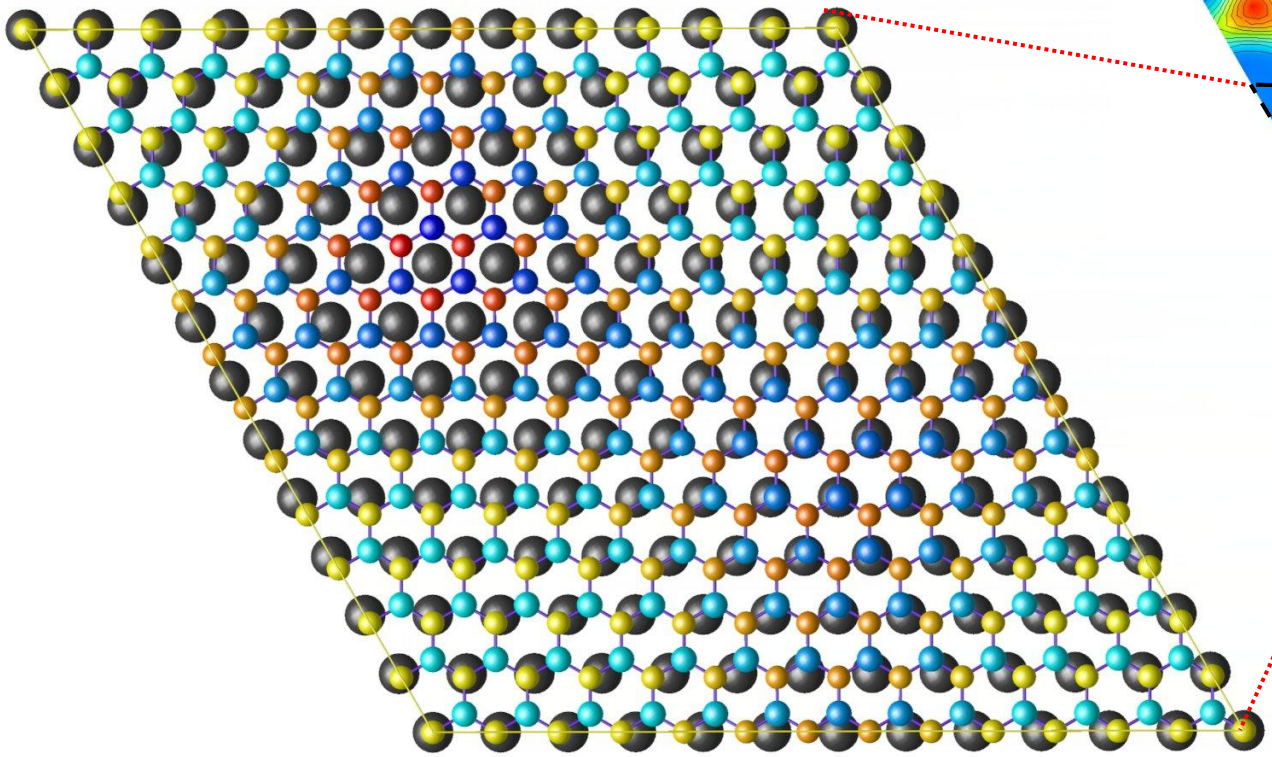

13 x 13 **BN**

12 x 12 **Rh**

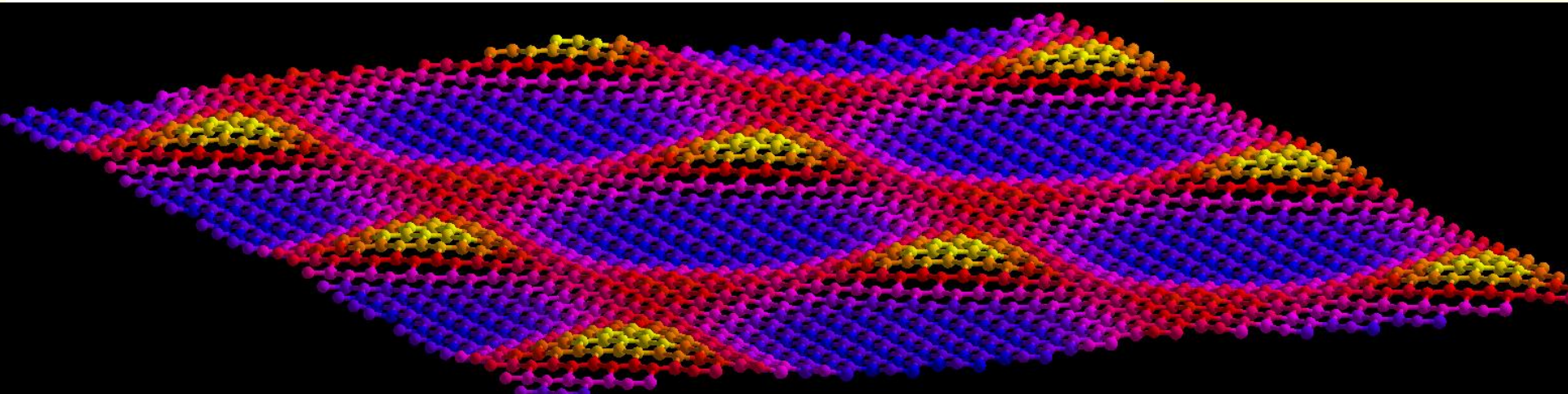

h-BN layer on Rh(111)

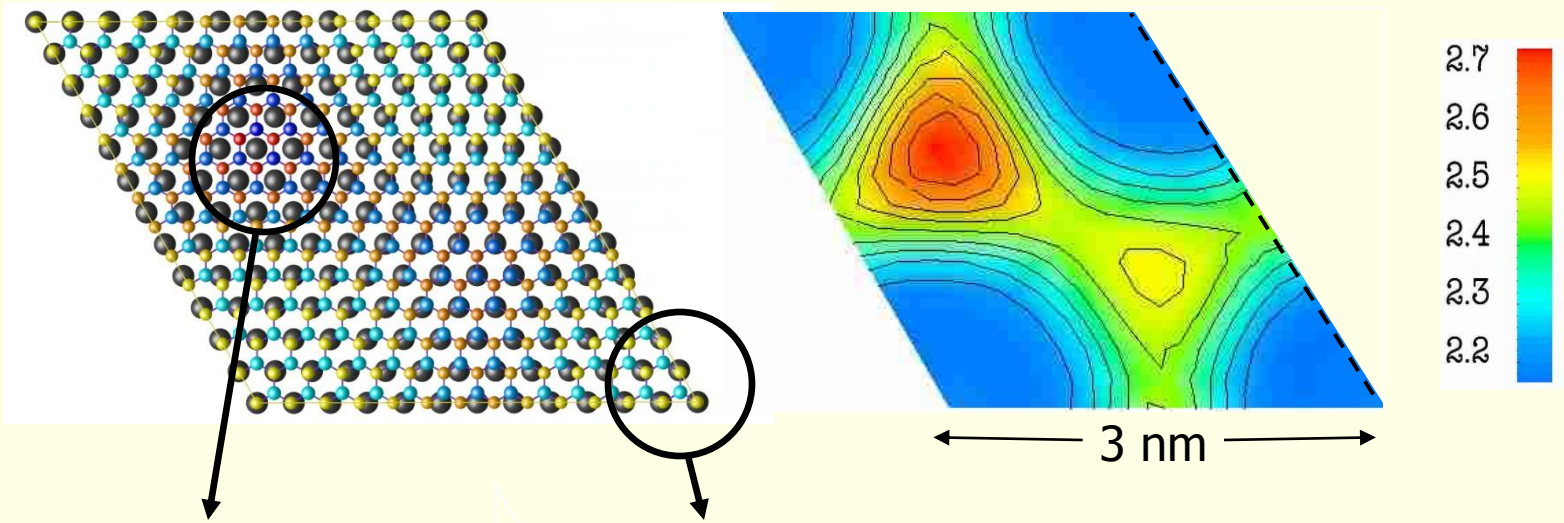

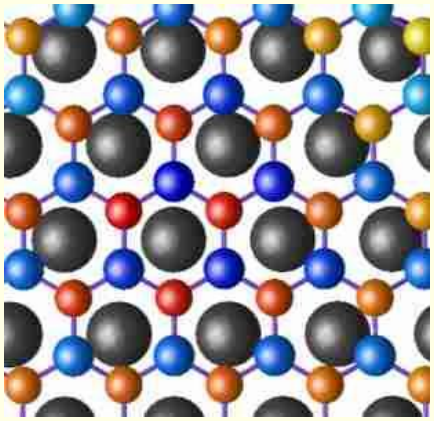

"high": "top" empty

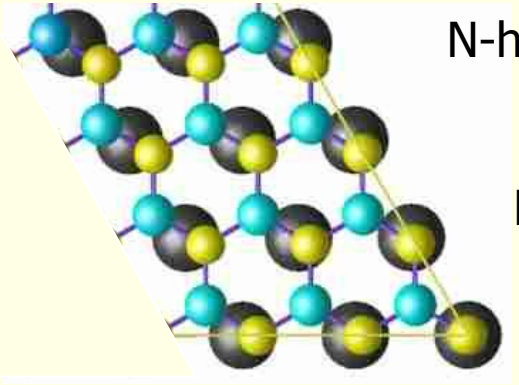

"low": N on "top"

N-high
B-high
N-low
B-low
Rh

R.Laskowski, P.Blaha, Th.Gallauner, K.Schwarz,
Single layer model of the h-BN nanomesh on the Rh(111) surface
Phys.Rev.Lett. 98, 106802 (2007)

Single h-BN layer on Rh(111)

distance of N from metal layer

as a function of xy position

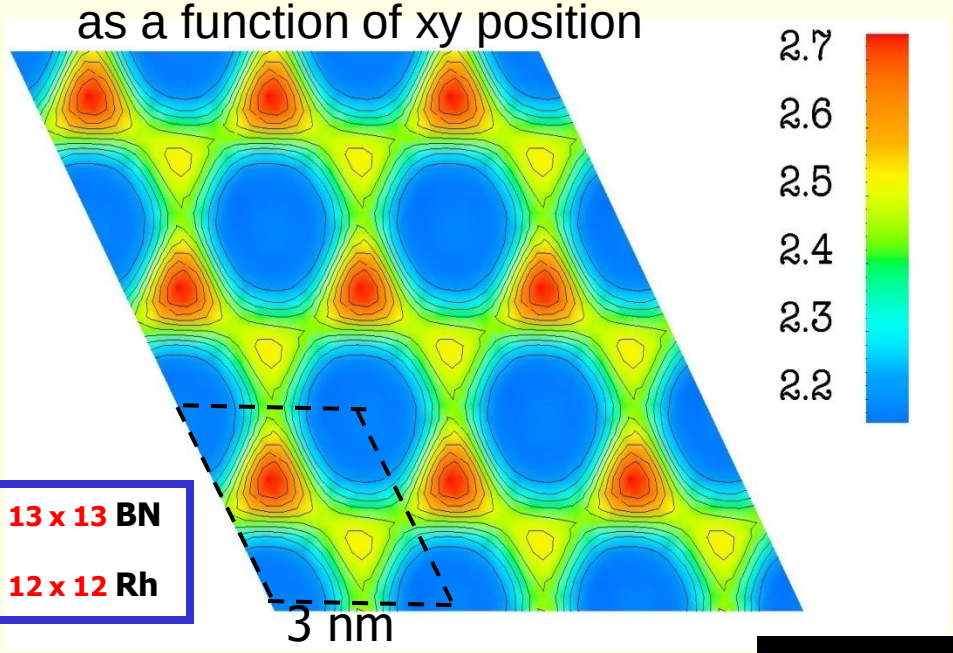

- h-BN layer is corrugated, amplitude=0.55 Å
- flat region of BN close to metal
- surrounding rims are made of two maxima with slightly different height
- E-total: - 4 187 608.963 Ryd

variation

enhanced side view

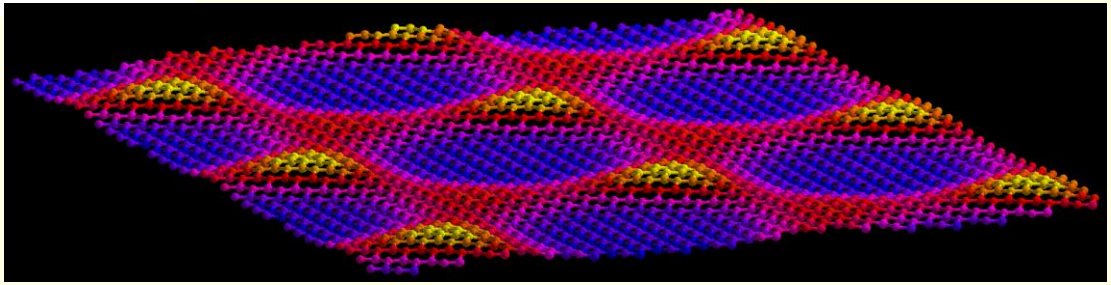

R.Laskowski, P.Blaha, Th.Gallauner, K.Schwarz,
Single layer model of the h-BN nanomesh on the Rh(111) surface
Phys.Rev.Lett. 98, 106802 (2007)

Force field vs. WIEN2k

- **3 layers Rh, h-BN on the both sides of the slab** (inversion symmetry)
- **12x12 Rh, 13x13 h-BN per layer (1108 atoms in the unit cell)**
- **Hamiltonian size ~50000** **metallic system !**
- **64 proc (Xeons), 2h per SCF iteration, 30 iterations/scf**

challenge for WIEN2k

N-metal layer distance

Force field

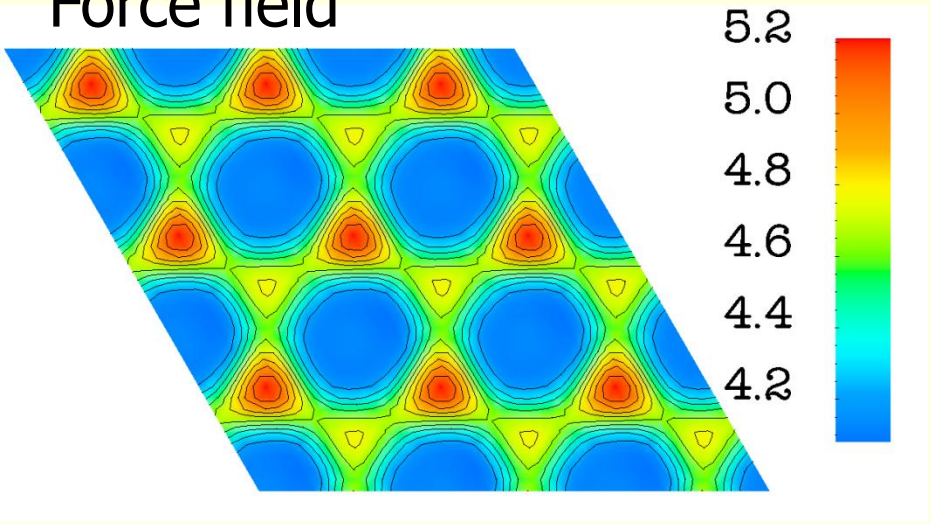

Wien2k

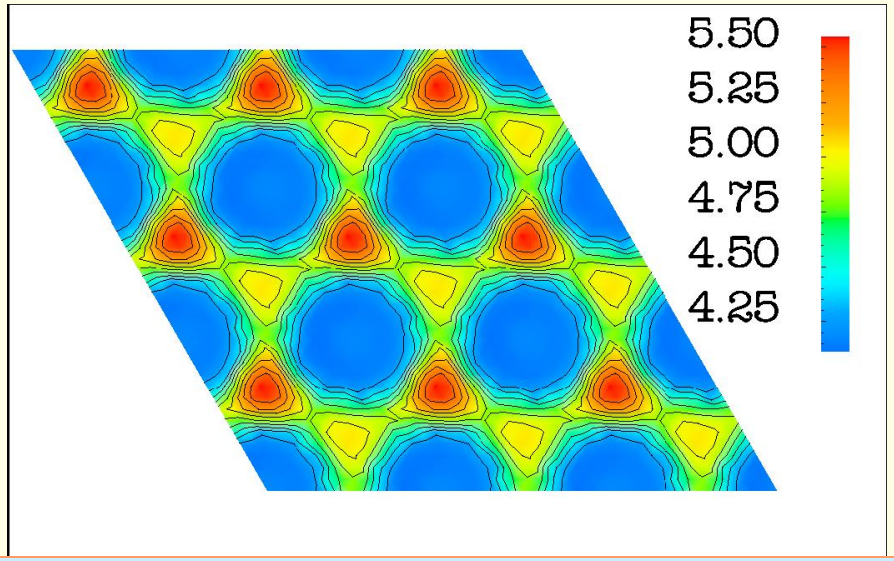

R.Laskowski, P.Blaha: *Unraveling the structure of the h-BN/ Rh(111) nanomesh by ab-initio calculations* J.Phys.Cond.Mat **20**, 064207 (2008)

Comparing STM images (Tersov-Hamann)

WIEN2k: -2 eV, 2A above surface

WIEN2k: + 2eV, 3A above surface

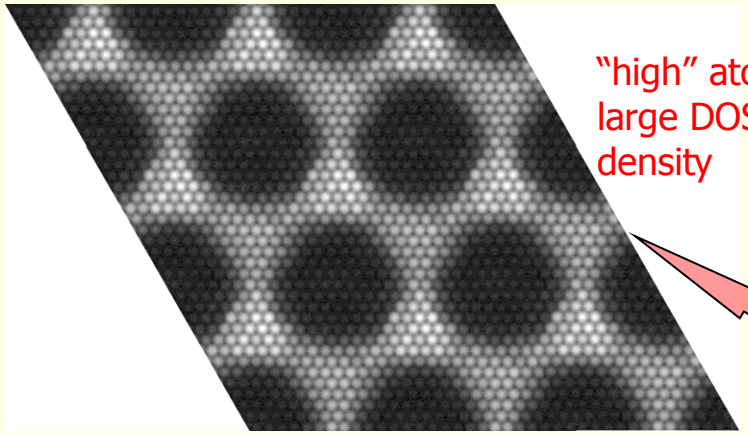

"high" atoms have large DOS and high density

"low" atoms have large DOS and high density

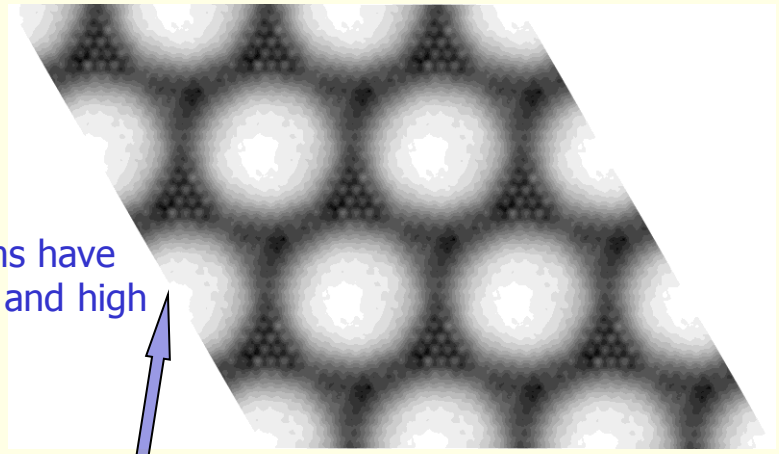

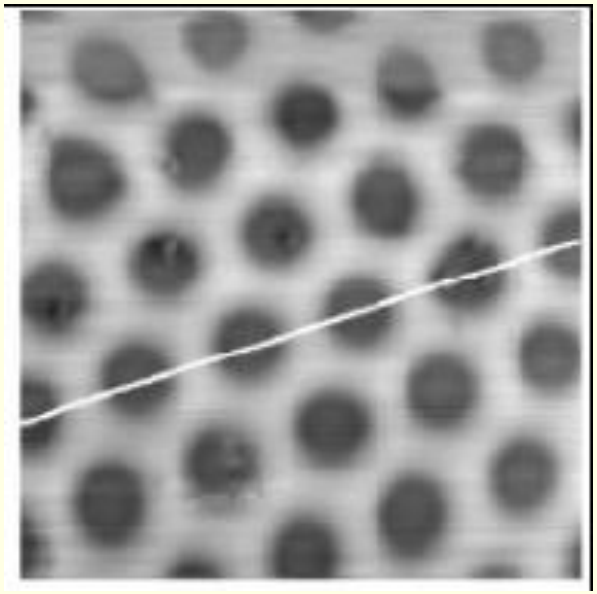

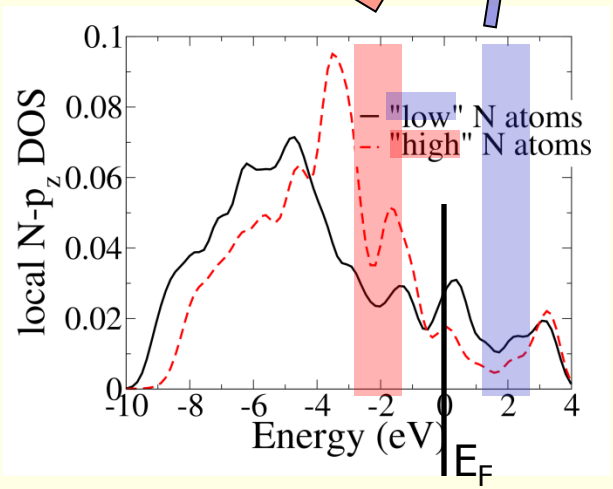

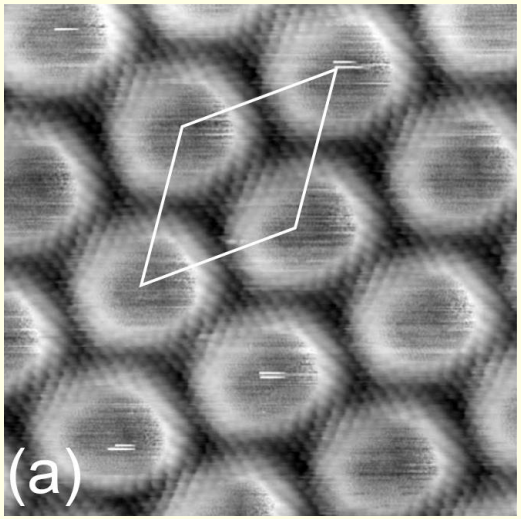

-2V: Goriachko et al., Langmuir **2007,** *23,* 2928

+0.07V: Preobrajenski *et al.* PRB **75**, 245412

single layer model of the h-BN/Rh(111) nanomesh

- single continuous BN layer: 13x13 BN on top of 12x12 Rh(111)

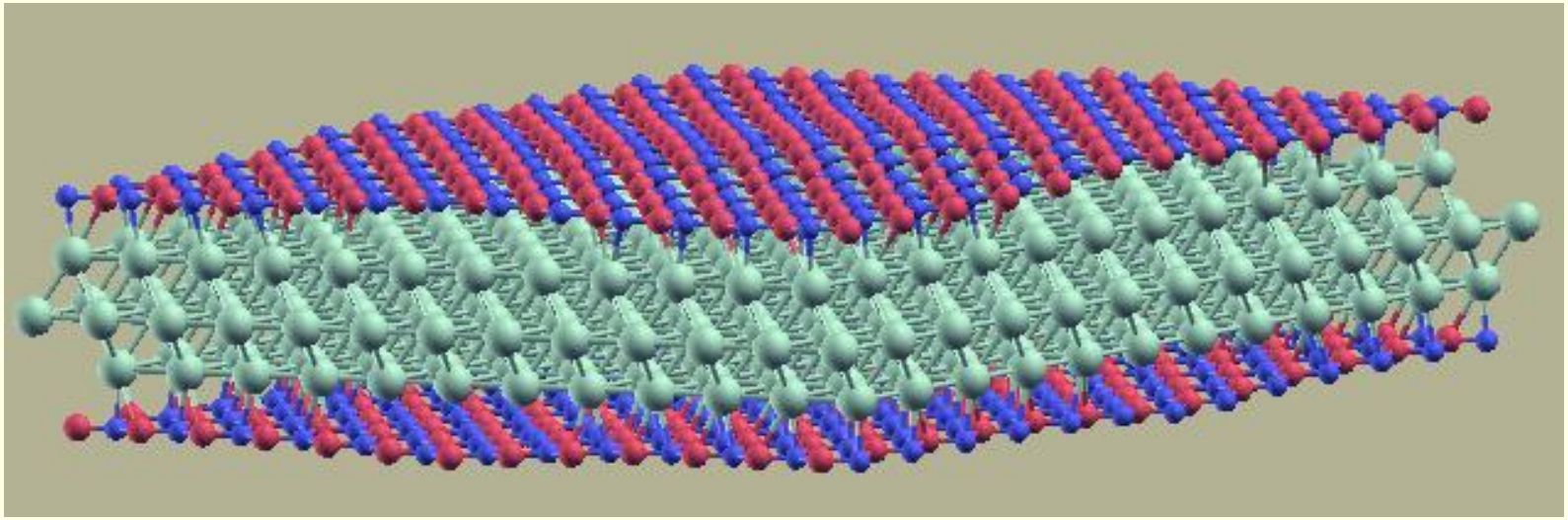

- DFT simulation:

  *quite **heavy**: 3 layers TM + BN: **1108** atoms/cell (**metal** !)*

  - ***WIEN2k*** *(all electron APW+lo full-potential calculations)*
    - **Hamiltonian size ~50000-70000 (50-100 GB memory)**
    - **64 proc (Xeons), 2h per SCF iteration, 30 iterations/scf**
    - **full structural optimization**

3. Example: Misfit layer compound

- Structure (model) $(PbS)_{1.14}TaS_2$
  of misfit layer compounds (MFLC)

- Mechanisms of stabilization
  predicted by experiment

- Computer simulations

Evgeniya Kabliman

E. Kabliman, P. Blaha, K. Schwarz,
Ab initio study of stabilization of the misfit layer coumpund $(PbS)_{1.14}TaS_2$
Phys.Rev.B 82, 125308 (2010)

The misfit layer compounds (MFLC)

Transition metal dichalcogenides (TMDCs)

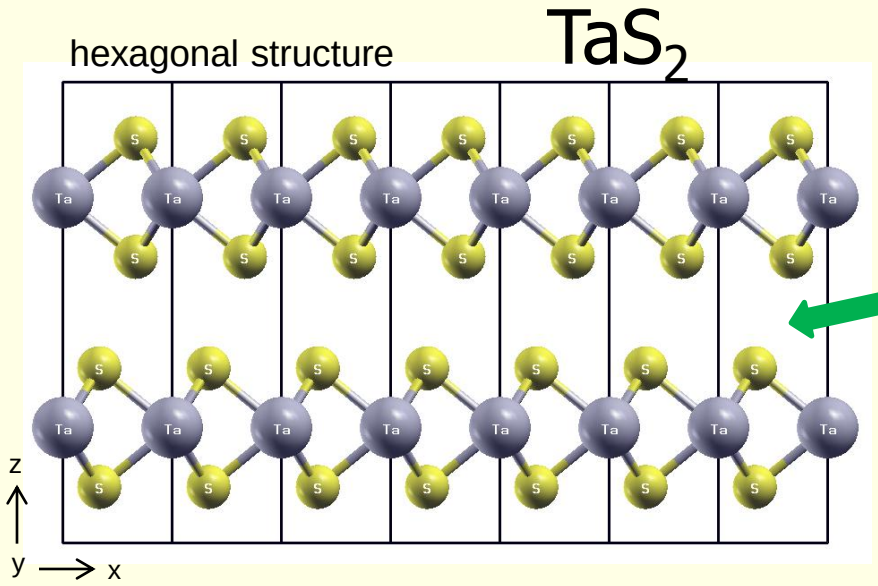

Cubic monochalcogenides (MCs)

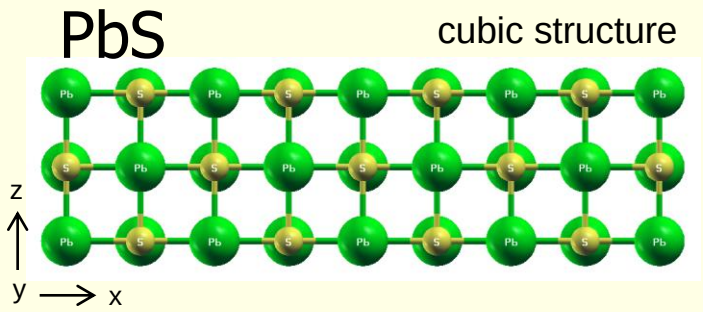

Misfit : x = $((2a_{TaS_2}/a_{PbS})-1)$

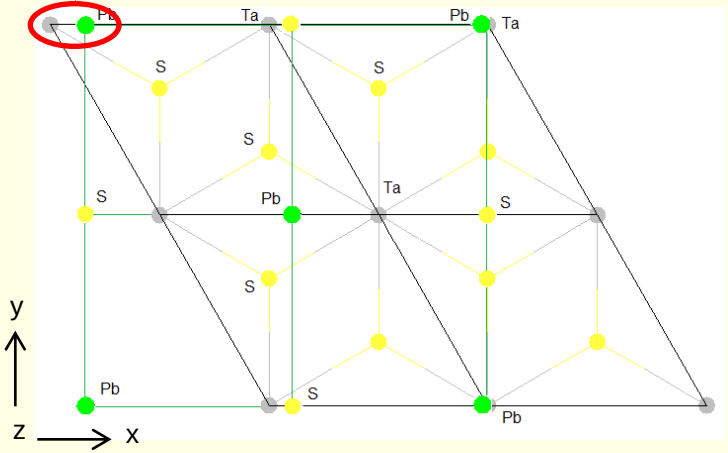

Interest

TMDCs – superconductivity and possibility of intercalating foreign atoms and molecules as well as double layers of cubic semiconductors *MX*.

The misfit layer compounds (MFLC)

$(MX)_{1+x}(TX_2)_m$

M = a metal atom Sn, **Pb**, Bi, Sb
or rare-earth one ;

X = a chalcogen atom **S** or Se ;

T = a transition metal atom Ti, V, Cr,
Nb or **Ta** ;

m = number of TX_2 layers between
two *MX* layers ;

m = (**1**,2,3) ;

x = $((2a_{TX_2}/a_{MX})-1)$; **- parameter of misfit!** ⟶ **Commensurate model of MFLC structure is needed**

$0.08 < x < 0.26$.

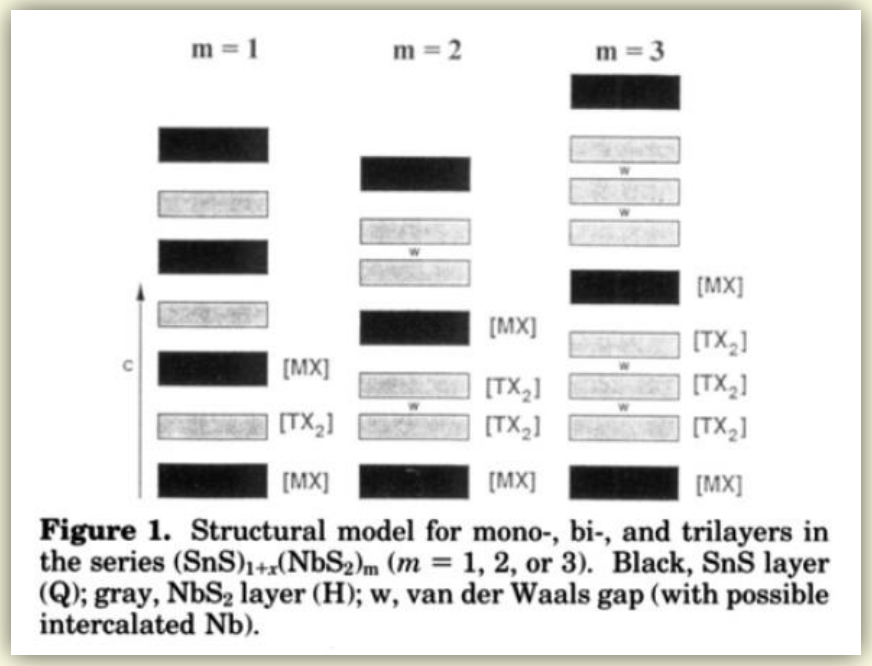

Figure 1. Structural model for mono-, bi-, and trilayers in the series $(SnS)_{1+x}(NbS_2)_m$ (m = 1, 2, or 3). Black, SnS layer (Q); gray, NbS_2 layer (H); w, van der Waals gap (with possible intercalated Nb).

Resonable numbers of *MX* and TX_2 unit cells

The misfit layer compound $PbS_{1.14}TaS_2$

Incommesurability in $(PbS)_{1.14}TaS_2$ is modeled by **"ideal" commensurate** periodic structure: **7** a_{TaS_2} **= 4** a_{PbS}

$$1+x = 8/7 = 1.14$$

Unit cell = **74** atoms in 19 Wyck. Pos.

TABLE II. The atomic coordinates of the fully relaxed $(PbS)_{1.14}TaS_2$ unit cell (stoichiometric and without cross substitution) in the *Bb2b* space group with a=23.19 Å, b=5.77 Å, and c =23.88 Å.

Atom	Wyck. pos.	x	y	z
Ta (1)	4*c*	0.2500	0.5789	0.2500
Ta (2)	8*d*	0.0360	0.0789	0.2504
Ta (3)	8*d*	0.6069	0.0788	0.2500
Ta (4)	8*d*	0.1787	0.0790	0.2497
S (1)	8*d*	0.0353	0.7454	0.3152
S (2)	8*d*	0.1784	0.7454	0.3147
S (3)	8*d*	0.6074	0.7459	0.3152
S (4)	8*d*	0.4647	0.7457	0.3147
S (5)	8*d*	0.3216	0.7453	0.3149
S (6)	8*d*	0.8925	0.7460	0.3152
S (7)	8*d*	0.7500	0.7462	0.3153
Pb (1)	8*d*	0.3128	0.9824	0.5660
Pb (2)	8*d*	0.5629	0.9921	0.5648
Pb (3)	8*d*	0.8123	0.9955	0.5643
Pb (4)	8*d*	0.0620	0.9868	0.5654
S (8)	8*d*	0.3125	0.4854	0.5488
S (9)	8*d*	0.5624	0.4923	0.5503
S (10)	8*d*	0.8125	0.4947	0.5510
S (11)	8*d*	0.0626	0.4885	0.5495

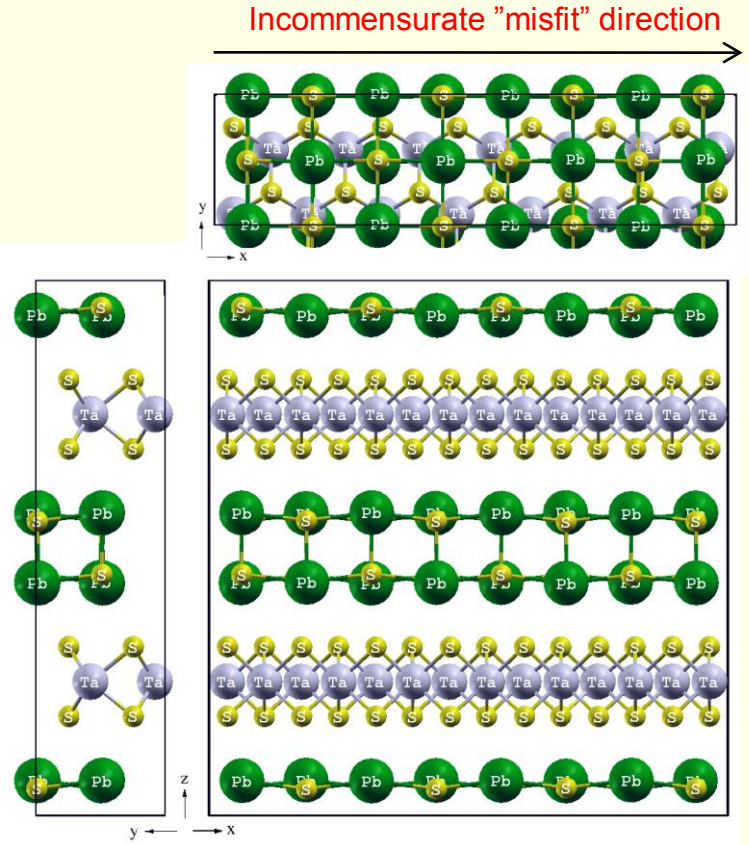

Figure 1. The conventional unit cell (a periodic structure containing 4 *PbS* and 7 TaS_2 unit cells in the incommensurate direction) of the stoichiometric $(PbS)_{1.14}TaS_2$ with relaxed "ideal" structure.

DFT simulation

Method

- DFT
- FP-LAPW+lo
- GGA (Wu Cohen 2006)

- R (Pb) = 2.80 a.u. ;
  R (Ta) = 2.13 a.u. ;
  R (S) = 2.07 a.u. ;
- $R_{min}K_{max}$ = 7.0 (plane wave basis set cutoff) ;
- N_k up to 2x2x5.

„Ideal" structure optimization

Compound	Space group	Parameters (Å)
PbS	$Fm\bar{3}m$	$a_{cubic}=a_{PbS}=5.91$ (5.914[a])
TaS_2	$P6_3/mmc$	$a_{hex}=a_{TaS_2}=3.30$ (3.314[b])
		$c_{hex}=c_{TaS_2}=12.097$ [b]
$(PbS)_{1.14}TaS_2$	$Bb2b$	$a=23.19$ (23.30/23.13)[c]
		$b=5.77$ (5.78)[c]
		$c=23.88$ (23.96)[c]

Formation energy

! $E_{form} \approx 0$ Ry

for stoichiometric $(PbS)_{1.14}TaS_2$
with relaxed "ideal" structure

WHAT stabilizes

misfit layer compounds ?

The misfit layer compound $PbS_{1.14}TaS_2$

?! **Two mechanisms of stabilization predicted by experiment :**

1. **Nonstoichiometry [1]** – a systematic cationic substitution of *M* ions by T atoms within the MX layer (necessary condition).

2. **Metal cross substitution [2]** – interchange of Pb and Ta atoms in the *PbS* and TaS_2 layers and nonstoichiometry **is not** a necessary condition.

Can theory find

the mechanism of stabilization.

for MFLC ?

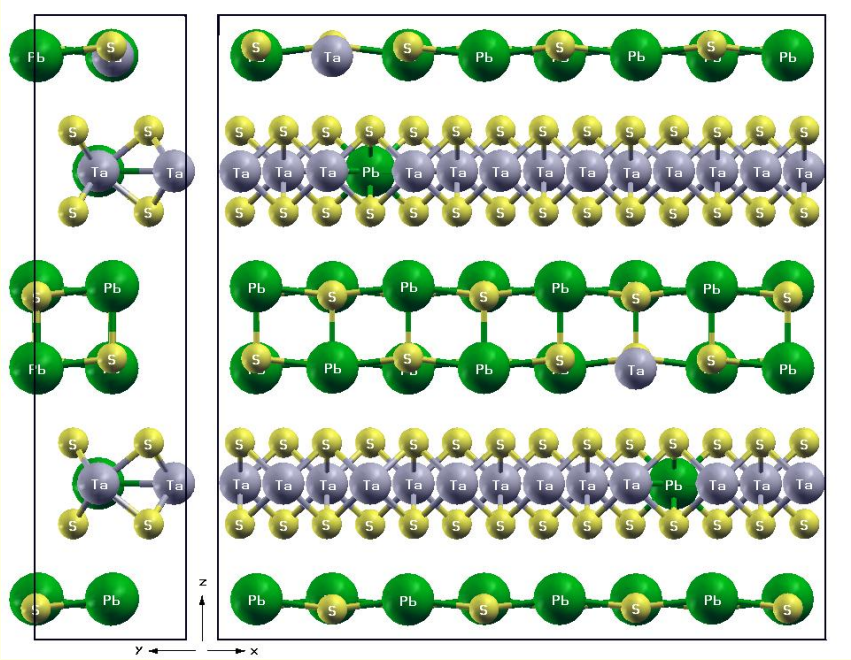

Figure 2a The conventional unit cell of the stoichiometric $(PbS)_{1.14}TaS_2$ compound with the lowest energy with a metal (Pb,Ta) cross substitution at a fairly small distance between the exchanged atoms.

[1] Y. Moëlo *et al*. Chem. Mat. 7, 1759 (1995)
[2] M. Kalläne *et al*. PRL 100, 065502 (2008)

Results: Energy of formation

$$E_{form} = E_{total}^{n_{Ta_{imp}}}((PbS)_{1.14}TaS_2) - \left[7 * E_{total}^{bulk}(TaS_2) + 4 * E_{total}^{bulk}(PbS) - n_{Ta_{imp}} E_{total}^{bulk}(Pb) + n_{Ta_{imp}} E_{total}^{bulk}(Ta)\right]$$

systematic metal substitution

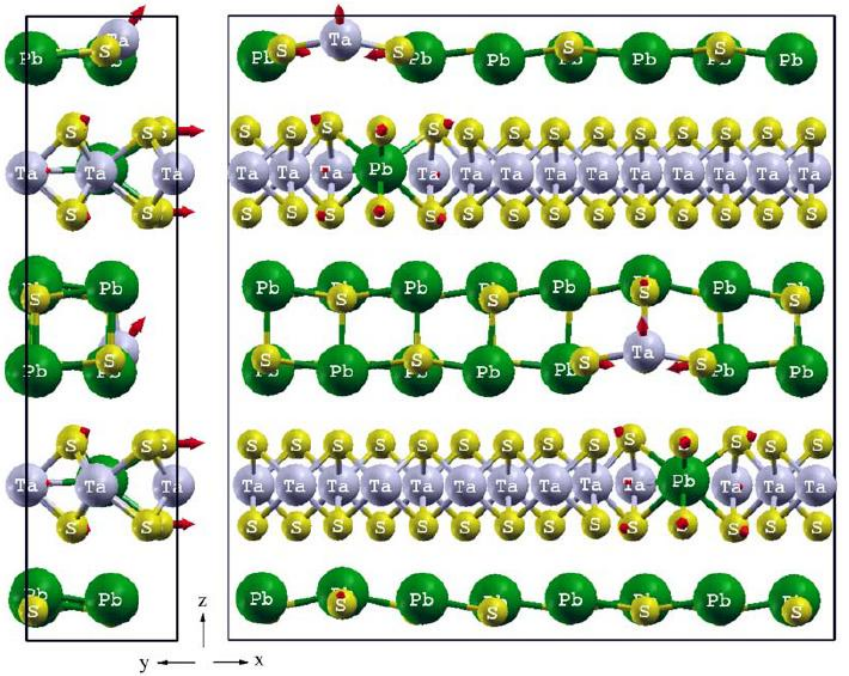

Figure 2b The $(PbS)_{1.14}TaS_2$ compound with the lowest energy relaxed structure after a metal (Pb,Ta) cross substitution.

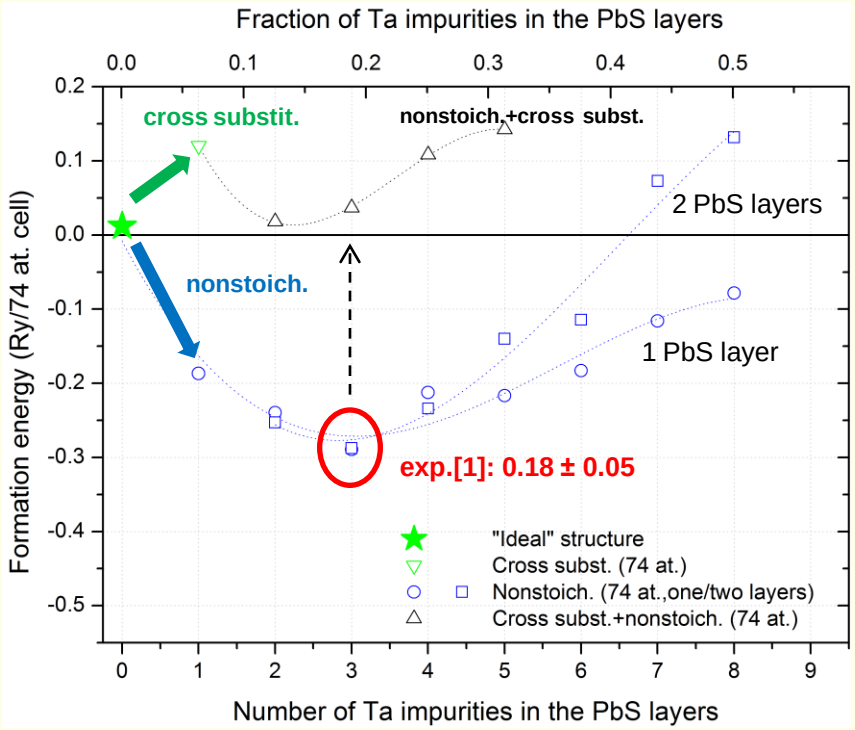

Figure 3a. The formation energy (Ry/74 at. unit cell) of $(PbS)_{1.14}TaS_2$. **74 atoms unit cell calculation.**

[1] M.Kalläne *et al*. PRL 100, 065502 (2008)

From 74 to 296 atoms per unit cell

(74 at. unit cell) x 4 → 296 atoms unit cell

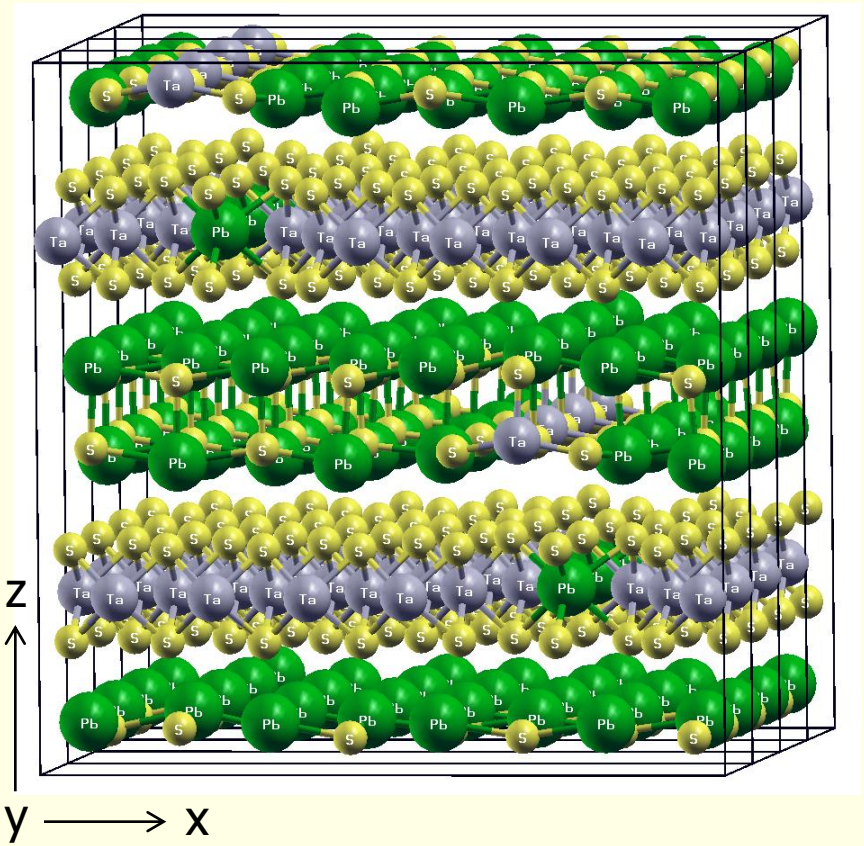

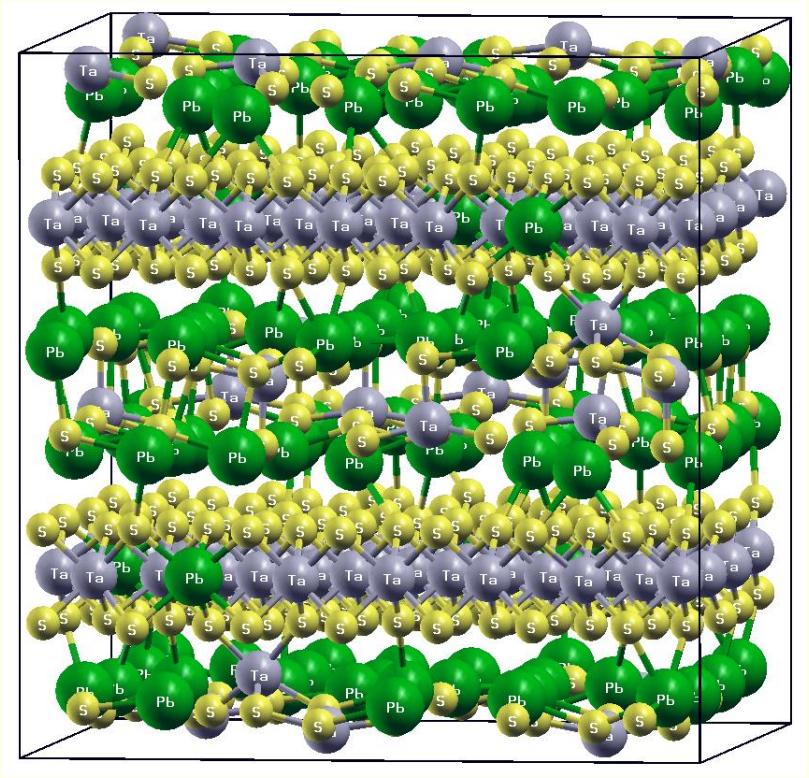

single metal substitution breaks the symmetry

Mechanism of stabilization of the misfit layer compound $(PbS)_{1.14}TaS_2$

Results: Energy of formation

- **Stabilization** of 0.4 Ry / 74 atoms cells for $n_{Ta_{imp}}$**=0.13-0.19** in a good agreement with experiment.
- **Nonstoichiometry** (Ta substitution in the pseudocubic *PbS* layers) is **necessary condition** for the stabilization of the $(PbS)_{1.14}TaS_2$ misfit layer compound.
- Pb impurities in the TaS_2 layer are also possible due to high T and non-equillibrium conditions during the growth of these materials.

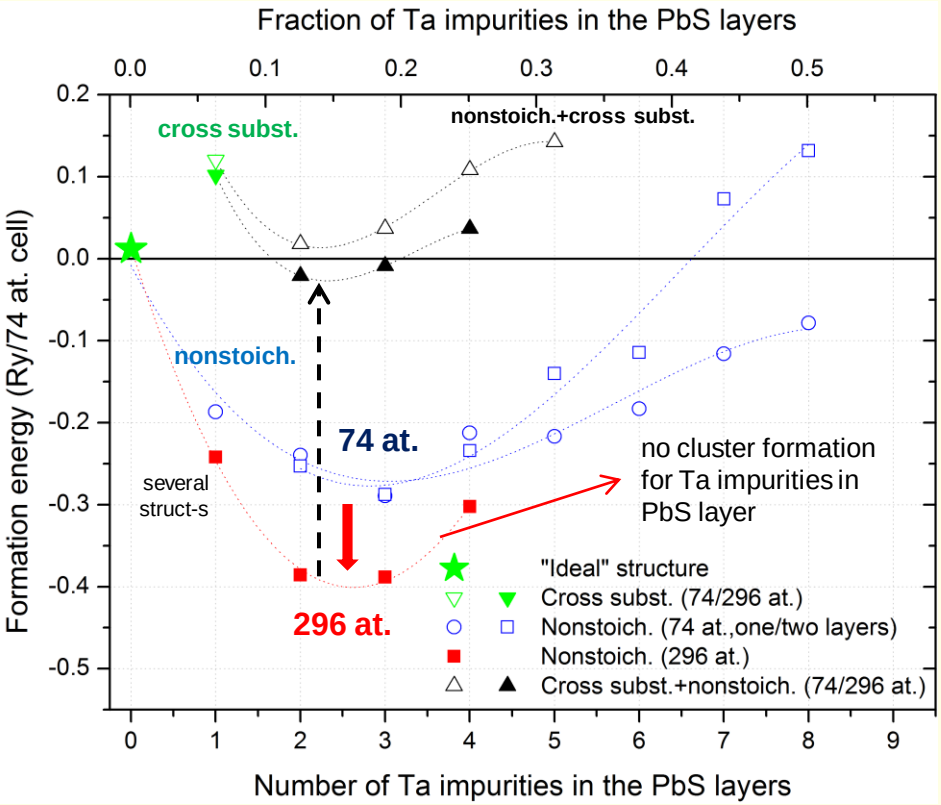

Figure 3b. The **formation energy** (Ry/74 at. unit cell) of $(PbS)_{1.14}TaS_2$. **74 and 296 atoms unit cell calculations.**

Results: Structure deformation

nonstoichiometry + metal cross substitution

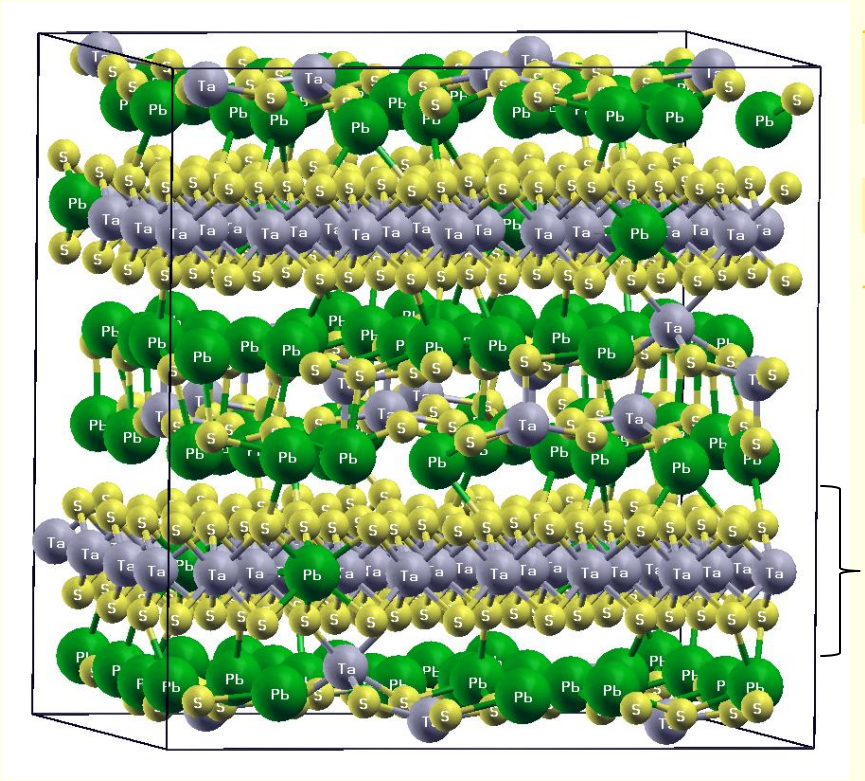

Change of atomic distances (Å) due to metal cross substitution and nonstoichiometry

	PbS	PbS layer (ideal)	TaS_2 (ideal)	TaS_2 layer (exch.)
Pb – S	2.957	2.74(z), 2.92(xy) 3.24 – 3.29[a]	-	2.69 – 2.76
Pb – Pb	4.182	4.05 – 4.22	-	-
Ta – S	-	-	2.46 - 2.47	2.44 – 2.50
Ta – Ta	-	-	3.32 - 3.33	3.15[b] – 3.60

no change

[a]Pb(*PbS*) – S(*TaS*$_2$); [b]Pb(exch) is nn-neighbour

"Breathing" of the *TaS*$_2$ layer:

Pb impurities change distances only to next nearest neighbours

Results: Structure deformation

nonstoichiometry + metal cross substitution

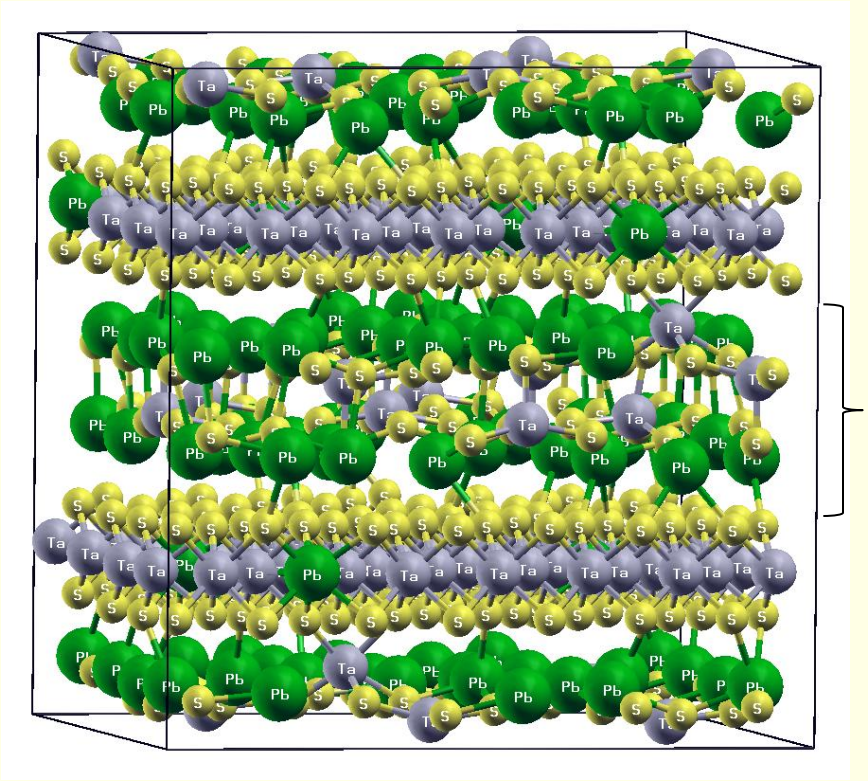

Change of atomic distances (Å) due to metal cross substitution and nonstoichiometry

	TaS_2	PbS layer (ideal)	TaS_2 (ideal)	PbS layer (exch.)
Pb – S	-	2.74(z), 2.92(xy) 3.24 – 3.29[a]	change →	2.74 – 3.04 3.07 – 3.71[a]
Pb – Pb	-	4.05 – 4.22	-	3.79 – 4.39
Ta – S	2.467	-	2.46 - 2.47	2.26 – 2.46
Ta – Ta	3.297	-	3.32 - 3.33	-

[a]Pb(*PbS*) – S(*TaS_2*)

Large distortion of *PbS* layer :

Ta impurities significantly change the interatomic distances

Results: Density of states

The parent compounds **The „ideal" $(PbS)_{1.14}TaS_2$**

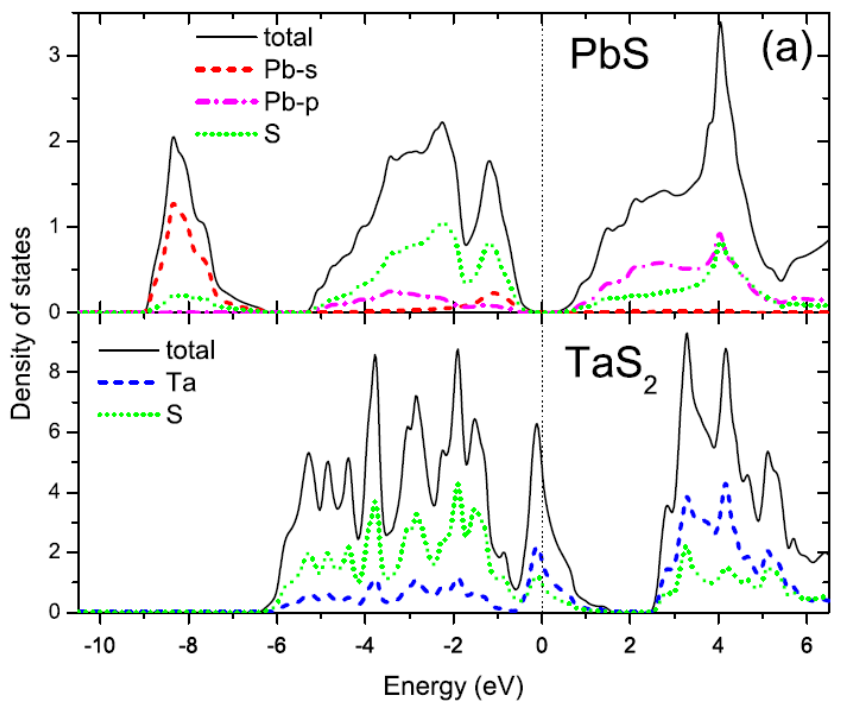

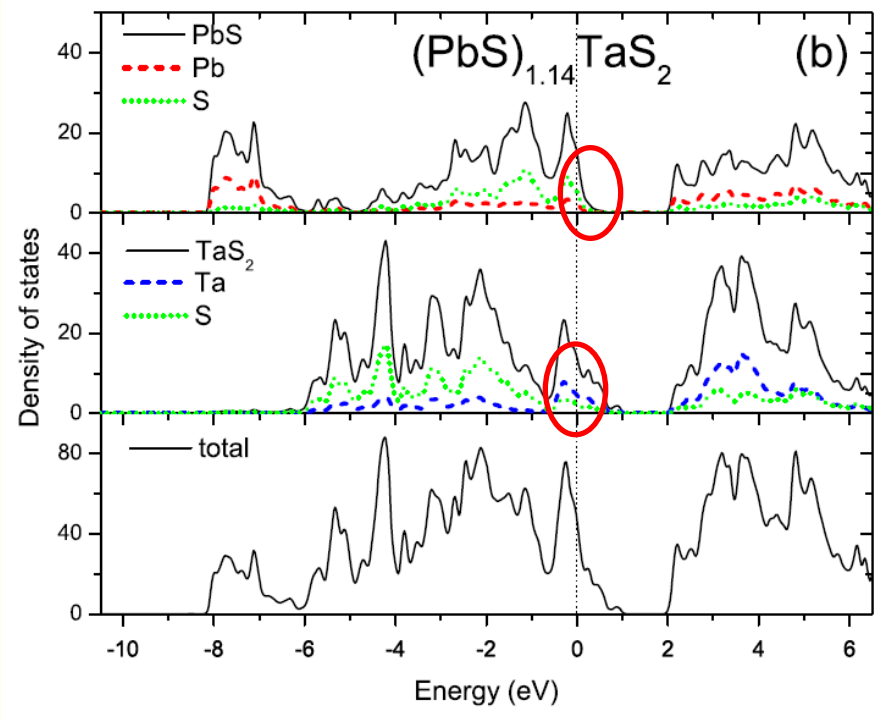

Charge transfer from PbS layer to TaS_2 layer

Results: Density of states

Nonstoichiometric model

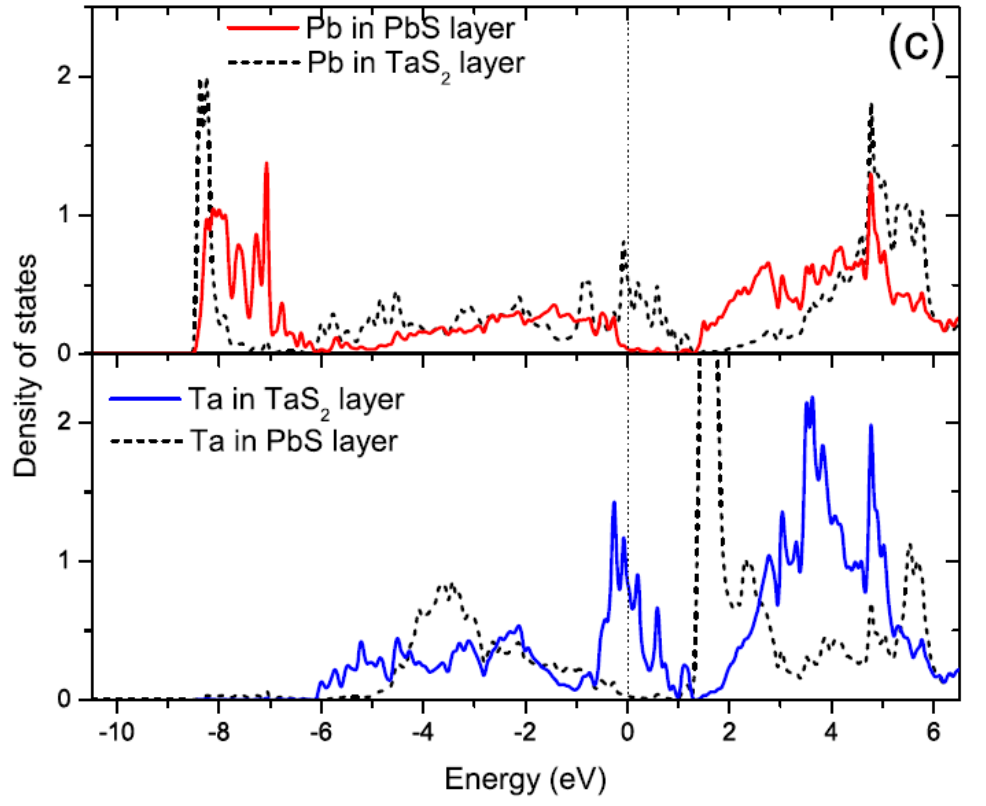

Why does nonstoichiometry improve the stability of MFLC?

- **Ta antisite** atoms restore the original "insulating *PbS*" DOS due to some charge transfer, but in addition only bonding Ta-d states (with S atoms) are occupied. The non-bonding Ta-d states are shifted above E_F.
- On the other hand, **Pb** antisite atoms are very compressed, have a metallic DOS at E_F and thus bring no stabilizing effect.

Results: XPS core level shifts

Experiment

- **about 2.15 eV** higher binding energies for **Ta-4f core anti-site states** with respect to Ta-4f host states in TaS_2
- **about 0.55 eV** lower binding energy for **Pb-5d anti-site states** respect to Pb-5d host states in *PbS.*

Calculation (Slater's transition-state)

- **about 0.9-1.5 eV** higher binding energies for **substituted Ta** atoms
- **about 0.2-0.5 eV** lower binding energy for **substituted Pb** atoms

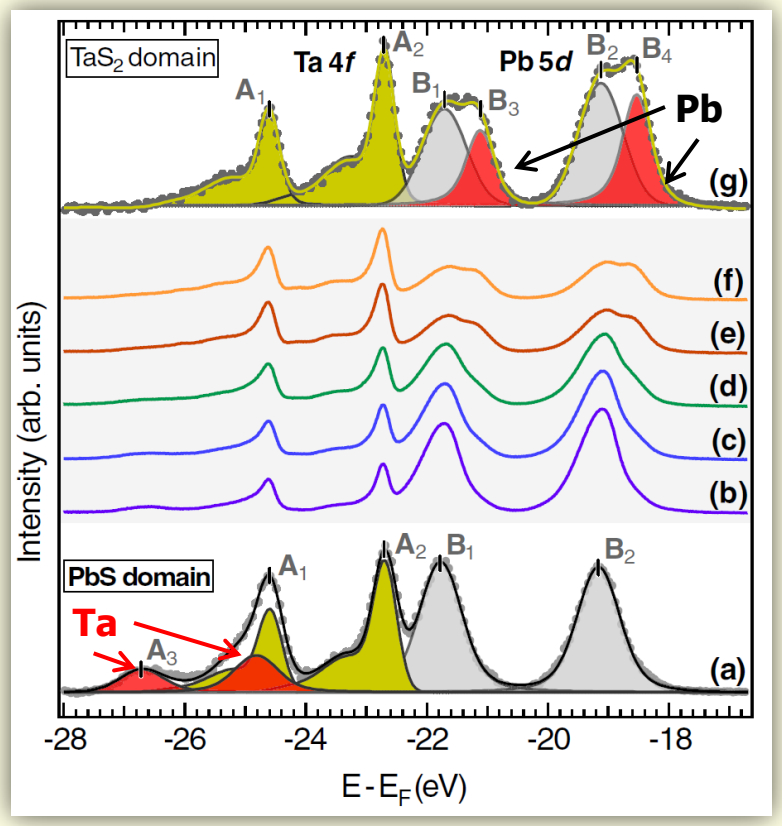

M. Kalläne *et al*. PRL 100, 065502 (2008)

Mechanisms of stabilization of $(PbS)_{1.14}TaS_2$

- ***The metal (Pb,Ta) cross substitution can not stabilize*** *the $(PbS)_{1.14}TaS_2$ compound according to the calculated formation energies.*
- ***The nonstoichiometric model*** *(Ta atoms substitute Pb in the PbS layer)* ***has a strong stabilizing effect*** *and thus must be the stabilizing mechanism in the misfit layer compounds.*
- ***The most stable structure*** *for an impurity concentration around* $n_{Ta_{imp}} = 0.15$ *in very good agreement with experimental estimates.*
- *Pb impurities in the TaS_2 layer are also possible due to high temperature and non-equilibrium conditions during the growth of these materials.*
- ***Large distortions of the flexible PbS layers****, when "small" Ta atoms are incorporated, but only a "breathing" , when Pb substitutes Ta in TaS_2.*
- *The stabilizing effect can be explained by analyzing* ***the DOS and the related charge transfer****.*
- *The* ***calculated XPS core level shifts*** *are in fairly good agreement with experiments.*

Summary

- DFT simulations with Wien2k
  - Atomic structure
  - Electronic structure
  - Properties
    - Relative stability (relaxations)
    - Electron (spin) densities
    - Magnetic order
    - Spectra
    - Comparison between theory and experiment
- Systems
  - Verwey transition (charged ordered vs. valence mixed) **$YFeBa_2O_5$**,
  - Nanomesh: **h-BN/Rh(111)**,
  - misfit layer compound **$(PbS)_{1.14}TaS_2$**

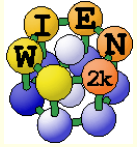

TU WIEN

Thank you for your attention !

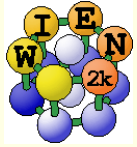

TU WIEN

Computational aspects

Increase in system size

- **WIEN2k** (APW+lo method)
  - Surfaces simulated with 3D-periodic slab geometry
  - unit cells with 1108 atoms (nanomesh),

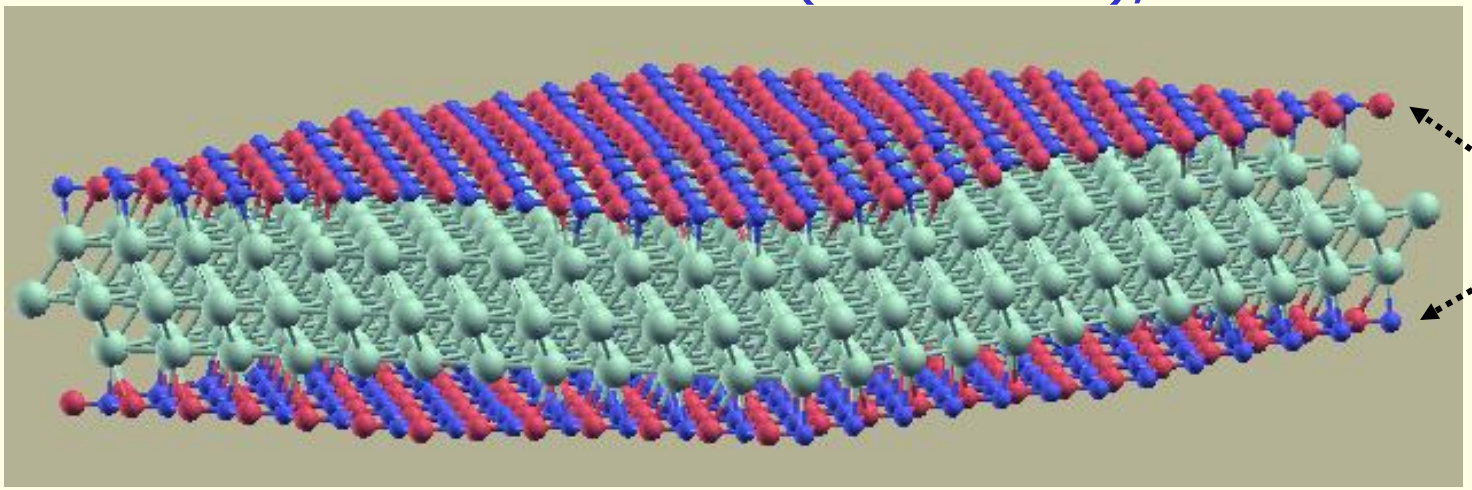

very expensive (matrix size: 50000x50000)
64 Xeons, 100 Gb memory, 3 days/geometry)

- **Scaling** from 1 atom/unit cell to 1000 atoms/u.c.

atoms	matrix size (N)	memory (N^2)	computer time (N^3)
1	N=50		
1000	N=50000	x 10^6	x 10^9

Aurora Cluster IBM e1350

- 72 x Dual Xeon
  3.6 GHz, 1MB L2
- FiberChannel Storage
  14 x 146GB-FC
- Infiniband Switch
  4 x SMC with 24 Gigabit-Ports

h-BN / Rh(111) nanomesh

STM Experiment: M.Corso et al., Science 303, 217(2004)
"partial double layer model"

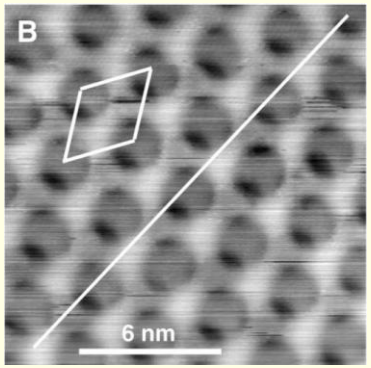

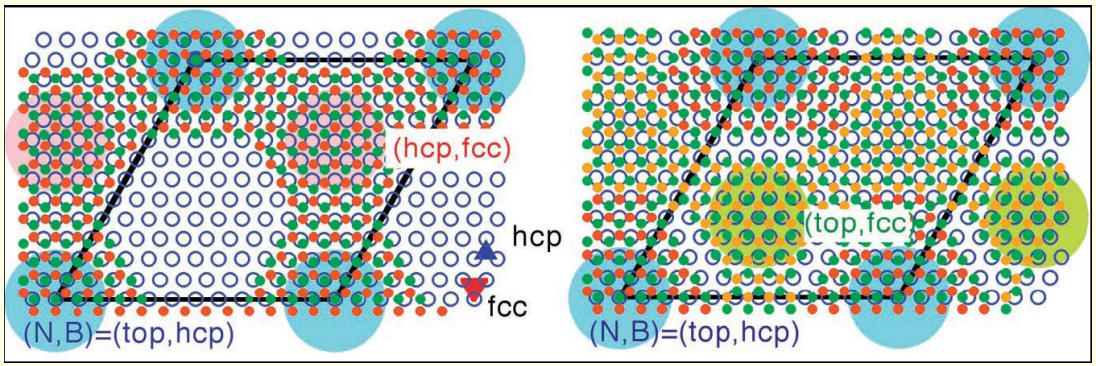

Theory: R.Laskowski et al., PRL 98, 106802 (2007):
"Corrugated single layer model"

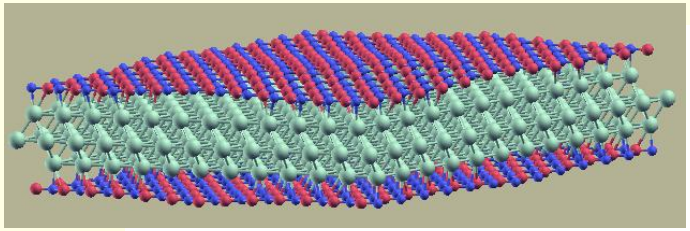

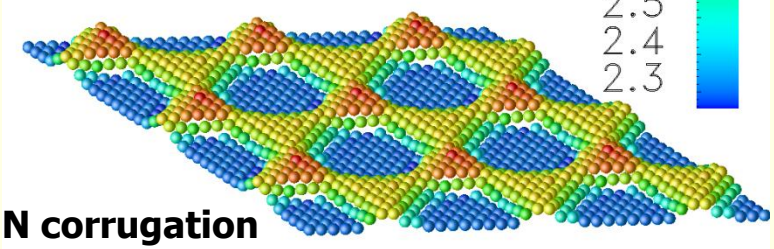

12x12 Rh, 13x13 BN, 1108 atoms/cell,

HC=ESC (50000x50000, 50 GB memory)
64 cpus, 2h/scf-cycle (was 20h!!)
3 month of computing time

Theoretical model was confirmed later !
H. Dill, et. al.: Science **319**, S. 1824(2008)

The breathing mode in $BaBiO_3$ (perovskite)

- Disproportionation

  $2\ Bi^{4+} \leftrightarrow Bi^{3+} + Bi^{5+}$

  the oxygen can be
  - *closer to Bi^{5+} (small octahedron, blue)*
  - *than to Bi^{3+} (large octahedron, yellow)*

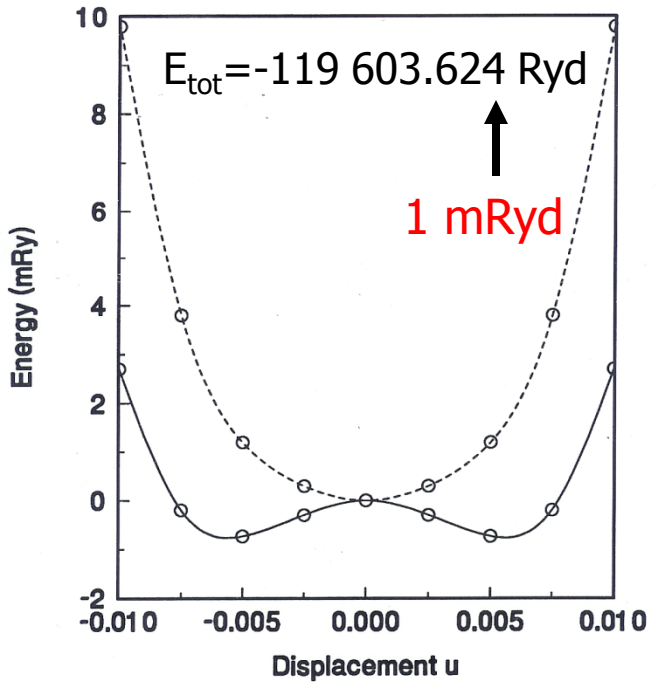

$Ba_{1-x}K_xBiO_3$

superconductor

Frozen phonon calculation

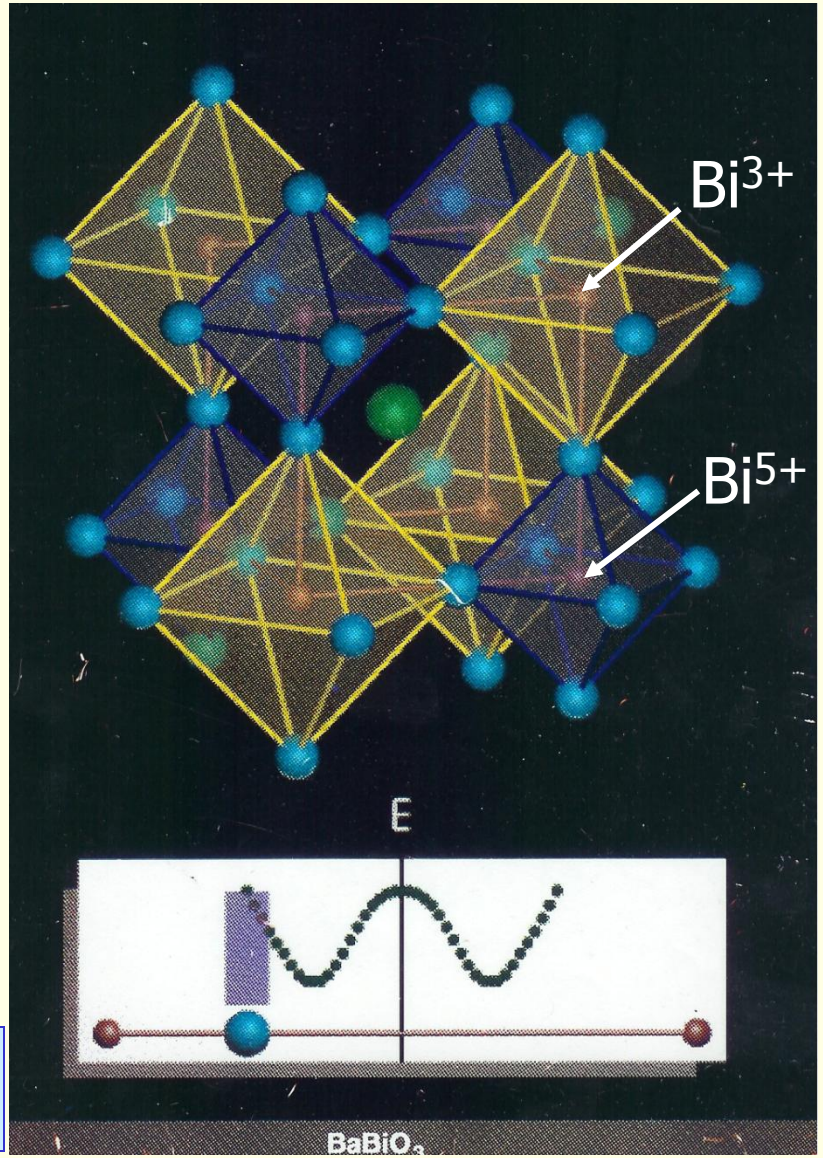

P.Blaha, K.Schwarz, Ph.Dufek. G.Vielsack, W.Weber: Z.Naturforsch. **48a**, 129 (1993)